NIH Public Access
Author Manuscript
J Cell Biochem. Author manuscript; available in PMC 2009 November 1.

Published in final edited form as:
J Cell Biochem. 2008 November 1; 105(4): 1008–1026. doi:10.1002/jcb.21901.

Migratory Activity of Human Breast Cancer Cells is Modulated by Differential Expression of Xanthine Oxidoreductase

Mehdi A. Fini[1,2], **David Orchard-Webb**[3], **Beata Kosmider**[4], **Jeremy D. Amon**[5], **Robert Kelland**[3], **Gayle Shibao**[1], and **Richard M. Wright**[1,2]

[1]Webb-Waring Institute for Cancer, Aging and Antioxidant Research, 4200 East 9th Ave, Denver, CO 80262

[2]The School of Medicine, Department of Pulmonary Sciences; University of Colorado Denver and Health Sciences Center, 4200 East 9th Ave, Denver, CO 80262

[3]Department of Biochemistry, University of Bath, Bath, U.K.

[4]National Jewish Medical and Research Center, 1400 Jackson Street, Denver, CO 80206

[5]Department of Biochemistry, Princeton University, Princeton, NJ

Abstract

Xanthine oxidoreductase (XOR) may exert an important, but poorly defined, role in the pathogenesis of breast cancer (BC). Loss of XOR expression was linked to aggressive BC, and recent clinical observations have suggested that decreasing XOR may be functionally linked to BC aggressiveness. The goal of the present investigation was to determine whether the decreased XOR observed in clinically aggressive BC was an intrinsic property of highly invasive mammary epithelial cells (MEC). Expression of XOR was investigated using HC11 mouse MEC, HB4a and MCF-10A normal human MEC, and several human mammary tumor cells including MCF-7 and MDA-MB-231. Consistent with clinical observations, data shown here revealed high levels of XOR in normal HC11 and MCF-10A cells that was markedly reduced in highly invasive mammary tumor cells. The contribution of XOR to tumor cell migration *in vitro* was investigated using MDA-MB-231 and MCF-7 cells and clonally selected derivatives of HC11 that exhibit either weak or strong migration *in vitro*. We observed that over-expression of an XOR cDNA in MDA-MB-231 and in HC11-C24, both possessing weak XOR expression and high migratory capacity, inhibited their migration *in vitro*. Conversely, pharmacological inhibition of XOR in MCF-7 and HC11-C4, both possessing high XOR expression and weak migratory capacity, stimulated their migration *in vitro*. Further experiments suggested that XOR derived ROS mediated this effect and also modulated COX-2 and MMP levels and function. These data demonstrate a functional link between XOR expression and MEC migration and suggest a potential role for XOR in suppressing BC pathogenesis.

Keywords

Xanthine Oxidoreductase; Breast Cancer; MCF-7; MDA-MB-231; COX-2; MMP1; MMP3; Migratory Activity

Address correspondence to: Dr. Richard M. Wright, University of Colorado Denver and Health Sciences Center, Campus Box C-322, 4200 East 9th Ave. Denver, CO 80262 Phone: 303 315 4593; Fax 303 315 8541; E-mail: richard.m.wright@uchsc.edu.

NIH-PA Author Manuscript
NIH-PA Author Manuscript
NIH-PA Author Manuscript

NIH-PA Author Manuscript

NIH-PA Author Manuscript

NIH-PA Author Manuscript

INTRODUCTION

Xanthine oxidoreductase (XOR) may exert an important, but poorly defined, role in the pathogenesis of breast cancer (BC). Loss of XOR activity has been linked to aggressive hepatic, renal, gastric, and mammary cancer [Linder et al., 2006; Linder et al., 2005]. In both mouse models of mammary carcinogenesis and in human BC patients decreasing mammary epithelial cell (MEC) XOR was associated with and/or predictive of poor clinical outcome and the degree of BC aggressiveness [Cook, 1997; Lewin et al., 1957; Linder et al., 2005; Shan et al., 2002]. Patients without evident epithelial XOR expression had the most aggressive BC and had 2.5 fold increased risk of recurrence compared with patients expressing normal or modestly reduced XOR [Linder et al., 2005]. A similar decline in serum XOR has been linked to aggressive stage in BC patients [Alsabti, 1980]. These data raise the possibility that down-regulation of XOR may be functionally linked to aggressive BC.

Although it is poorly expressed in virgin mammary glands [McManaman et al., 2000], XOR is an abundant milk protein and it is highly expressed in mammary tissue during pregnancy and lactation [Anderson et al., 2007; Garattini et al., 2003; Linder et al., 1999] where it plays an important functional role in lactation and differentiation of MEC [Anderson et al., 2007; Kurosaki et al., 1996; Linder et al., 1999; McManaman et al., 2000; McManaman et al., 1999; McManaman et al., 2002; Seymour et al., 2006]. Heterozygous XOR knockout mice (XOR+/−) exhibit disrupted formation of the milk fat globule [Vorbach et al., 2002], and recent data demonstrate that XOR forms a sulphydryl-bond-dependent complex with butyrophilin (Btn) and adipophilin (ADPH) in the milk fat globule membrane. This functional interaction between XOR, Btn, and ADPH appears to be essential for the formation of the milk fat globule during lactation [Anderson et al., 2007; McManaman et al., 2002].

While XOR may contribute to alcohol induced BC pathogenesis and carcinogenesis [Castro et al., 2007; Maciel et al., 2004; Wright et al., 1999], the potential for XOR down-regulation to contribute to BC aggressiveness is unknown. XOR is a member of the molybdoflavo-proteins that catalyzes the formation of uric acid from xanthine and hypoxanthine. During purine oxidation XOR is a source of reactive oxygen species (ROS) that have been implicated in numerous human diseases [Garattini et al., 2003]. Both H_2O_2 and $O^{-\cdot}{}_2$ are ROS produced from XOR following conversion of D-form XOR to O-form XOR, and in most cells expressing XOR approximately 40% of the native enzyme is in O-form [Garattini et al., 2003]. XOR also possesses two potentially relevant catalytic functions in addition to purine oxidation. Recent evidence indicates that XOR can convert nitrites into nitric oxide (NO), contributing to the formation of peroxynitrite and perhaps other reactive nitrogen species (RNS) [Godber et al., 2000; Li et al., 2004; Millar, 2004]. XOR is also a highly efficient ROS generating NADH oxidase [Maia et al., 2007; Maia et al., 2005; Sanders et al., 1997], and this catalytic function cannot be inhibited by the substrate analogs allopurinol or oxypurinol. Furthermore, uric acid, the product of purine oxidation by XOR, is itself a well recognized scavenger of peroxynitrite and hydroxyl radical [Becker, 1993; Hooper et al., 2000; Kean et al., 2000]. As a source of intracellular ROS, RNS, or uric acid XOR could potentially regulate many aspects of MEC function or signaling that could modulate BC pathogenesis, including regulation of cyclooxygenase-2 (COX-2) [Ohtsubo et al., 2004], hypoxia inducible factor-1α (HIF-1α) [Griguer et al., 2006], peroxisome proliferator activator receptor-γ (PPAR-γ) [Cheung et al., 2007], NF-κB [Matuschak et al., 2004], or other unknown factors.

ROS may have widely divergent effects on cancer cell migration and cancer pathogenesis. On the one hand ROS have been reported to stimulate cancer cell or smooth muscle cell

NIH-PA Author Manuscript

NIH-PA Author Manuscript

NIH-PA Author Manuscript

migration by activating protein kinase-C (PKC) and the ERK MAP Kinase [Lo et al., 2005; Wu et al., 2006], and this may be responsible for tumor progression in certain tumors [Storz, 2005; Wu, 2006]. However, as noted elsewhere "the mechanism by which cells respond to reactive oxygen species depends on the molecular background of cell and tissues, the location of ROS production, and the concentration of individual ROS species" [Storz, 2005]. Indeed, elevation of ROS levels in some cancer cells appeared to inhibit migratory activity, while scavenging of ROS stimulated migratory activity [Shim et al., 2006]. As an intracellular source of ROS, XOR may be anticipated to affect migratory activity of cancer cells, although it is uncertain how this effect would unfold.

The goal of the present investigation was to determine whether the decreased XOR observed in clinically aggressive BC was an intrinsic property of highly invasive mammary cancer cells. Data shown here have, for the first time, demonstrated vigorous XOR expression in normal or weakly invasive MEC that is lost in highly invasive MEC. Furthermore, over-expression of recombinant XOR cDNA in highly invasive MEC inhibits their migration *in vitro*, whereas pharmacological inhibition of XOR in MEC possessing high XOR activity and weak migratory activity induces their migration *in vitro*. Present experiments indicate that XOR derived ROS as well as modulation of COX-2 levels and the levels and function of matrix metaloproteases-1 and -3 (MMP-1, -3) may be involved in the suppressive effect of XOR on MEC migration.

MATERIALS AND METHODS

Reagents

Most reagents, buffers, substrates, PAGE supplies, and EGF were purchased from Sigma Chemical Company (St Louis, MO, USA). Media for cell culture were obtained from Gibco/BRL (Bethesda, MD, USA). Insulin, was purchased from Sigma-Aldrich (St. Louis, MO, USA). Fetal bovine serum was from Gemini Bioproducts (Woodland, CA, USA). Oligonucleotides were synthesized by Integrated DNA Technology (Coralville, IA, USA). The pGL3 luciferase fusion plasmids and beta galactosidase expressing plasmid pcDNA3.1(+)-HisMycLacZ were obtained from Promega (Madison, WI, USA). The Topo-II T:A cloning vector was obtained from Invitrogen (Carlsbad, CA, USA). O-nitrophenyl beta-D galactopyranoside, and restriction endonucleases were obtained from Roche Molecular Biochemicals (Indianapolis, IN, USA). BAC26F21 was obtained from Research Genetics (Huntsville, AL, USA). MMP inhibitors I and III were purchased from EMD Chemicals, Inc. (Gibbstown , NJ, USA). The following primary antibodies were used: monoclonal mouse anti-α-Smooth Muscle Actin (A2547, Sigma), rabbit anti-βactin (A-2066, Sigma). Rabbit antibody to XOR (100−4183) was obtained from Rockland, Inc. (Gilbertsville, PA, USA). Human reactive anti-MMP1 (sc-30069) and anti-MMP3 (sc-30070) were purchased from Santa Cruz Biotechnology, Inc. (Santa Cruz, CA, USA). The following antibodies were used for fluorescent labeling: FITC conjuagated Donkey anti-Rat IgG (712−095−150, Jackson ImmunoResearch, West Grove, PA, USA), FITC conjugated Donkey anti-Mouse IgG (715−095−150, Jackson ImmunoResearch). The following Horse Radish Peroxidase conjugated secondary antibodies were used in western blots: goat anti-rat IgG (sc-2006, Santa Cruz), Goat anti-mouse IgG (sc-2005, Santa Cruz), and Goat anti-rabbit IgG (sc-2004, Santa Cruz).

Cells and culture conditions

HC11 mouse MEC were grown in RPMI 1640 containing 2mM l-glutamine, 2g/l sodium bicarbonate, pH 7.4, 1X of antibiotic/antimycotic solution, 5ug/ml insulin, 10ng/ml epidermal growth factor, 10% fetal calf serum [Hynes et al., 1990]. Cells were maintained at 37°C in 95% air/5% CO_2, fed every 2 days, and split 1:4 when at, or near, confluency.

NIH-PA Author Manuscript

NIH-PA Author Manuscript

NIH-PA Author Manuscript

MCF-10A and Hb4a normal human MEC were grown as described [Page et al., 1998] with minor modifications as follows. Medium consisted of RPMI 1640 containing 2mM l-glutamine, 2g/l sodium bicarbonate, pH 7.4, 1X of antibiotic/antimycotic solution, 5ug/ml insulin, 5ug/ml hydrocortisone, 100ng/ml cholera toxin, and 10% fetal calf serum. Cells were maintained at 37°C in 95% air/5% CO_2, fed every 2 days, and split 1:4 when at, or near, confluency. T47D cells were grown in RPMI 1640 containing 2mM l-glutamine, 2g/l sodium bicarbonate, pH 7.4, 1X of antibiotic/antimycotic solution, 5ug/ml insulin, and 10% fetal calf serum. All other cancer cell lines were grown in DMEM (high glucose) containing 2mM l-glutamine, 2g/l sodium bicarbonate, pH 7.4, 1X of antibiotic/antimycotic solution, 5ug/ml insulin, and 10% fetal calf serum [Larkins et al., 2006]. Cells were maintained at 37°C in 95% air/5% CO_2, fed every 2 days, and split 1:3 when at, or near, confluency. All human cancer cells were obtained from the ATCC.

XOR Quantitation

Total XOR activity was determined at 293nm by quantitation of oxypurinol inhibitable uric acid synthesis using a Cary spectrometer, 1cm path length, and a molar extinction coefficient for uric acid of 12,600M^{-1} as previously described [Seymour et al., 2006].

SDS-PAGE and western immunoblot analysis

Cells to be used in immunoblot analyses were washed twice with ice-cold PBS, resuspended in RIPA lysis buffer (50mM Tris-base pH 8.0, 150mM NaCl, 1% NP-40, 0.2% SDS, 25mM EDTA, 2mM DTT, 10mM NaF, and 10mM Na3VO4; PMSF, aprotinin, leupeptin, and pepstatin were added at 1mM immediately prior to use), sedimented at 10,000 rpm for ten minutes at 4°C, the supernatants isolated and kept on ice. Protein concentration in the supernatant was determined using the bicinchoninic acid assay (Sigma-Aldrich). Aliquots containing 50μg of protein were incubated with equal amounts of loading buffer (5 % β-mercaptoethanol, 95% Laemmli loading dye) for 10 mins at 37°, then boiled for 5 mins. Samples were then separated by electrophoresis on 7.5% SDS-PAGE or 4% to 20% gradient SDS-PAGE gels for 40 mins at 100V, transferred to PVDF membranes (Whatman, Inc, AL, USA). Membranes were blocked overnight at 4° in 5% non-fat dried milk in Tris-buffered saline (pH 7.6) containing 0.1% Tween. Membranes were then incubated with antibodies as indicated. Antigen-antibody complexes were detected by reaction with an ECL Western blotting detection kit according to manufacturer's instruction (Amersham Life Sciences, Piscataway, NJ, USA). Each experiment was run in duplicate or triplicate, and representative immunoblots are shown.

Human XOR upstream DNA cloning, deletion construction, and expression

Upstream DNA from the human XOR genomic locus was obtained using the bacterial artificial chromosome (BAC) clone BAC26F21 (accession number AL121654; gi 6002387). DNA was prepared as described by the clone's supplier, Research Genetics (Huntsville, AL, USA). XOR upstream DNA, including the previously identified basal promoter [Xu et al., 1996; Xu et al., 2000], was amplified from BAC26F21 by PCR as described previously [Roberts et al., 2007; Wright et al., 2000]. Briefly, upstream DNA was amplified using the 5’ primer hXDHP1 5’-ATCAAA**CTCGAG**GACATTCATTGTTGTTCATTTTATTGGGGTGG-3’ which incorporates an Xho-I cleavage site (bold) 5’ of the XOR sequence. This was paired to the primer hXDHCON 5’-GAAAACCAATTTGTCTGCTGCCATGGTCACAGGGTGGGGTC-3’ which introduces two nucleotide substitutions in the human XOR DNA (CAATGA) that convert the translational start site of XOR into an Nco1 site (CCATGG) and allows subsequent fusion to the translational start site of the luciferase gene in the pGL3-Basic expression vector. The resulting 1.9kbp PCR product was cloned into the TopoII vector and sequenced from both

NIH-PA Author Manuscript

NIH-PA Author Manuscript

NIH-PA Author Manuscript

directions, generating the clone phXDPRO-1.9. The resulting sequence was identical to that for BAC26F21 and to the previously reported XOR upstream DNA [Xu et al., 1996]. DNA cloned in TopoII was excised by Xho-1 and Nco-1 cleavage and cloned into pGL3-Basic to generate the clone phXD-B1. Potential transcription factor binding sites were identified by the TESS multifactorial detection software (www.cbil.upenn.edu/cgi-bin/tess/) and the TRANSFAC 4.0 database which confirmed the location of previously identified transcription factor binding [Xu et al., 1996].

Ten in-frame deletion fusions to the translational start site of the luciferase gene in the pGL3-Basic (pGL3-B; Promega) were constructed in steps of 200 bp as indicated previously [Clark et al., 1998a; Clark et al., 1998b; Roberts et al., 2007; Wright et al., 2000]. Upstream DNA deletions to be cloned in pGL3-B were amplified by PCR using phXDPRO-1.9 as a template for PCR. Upstream primers were paired to 3’ primer, hXDHCON. The resulting PCR products were cleaved with XhoI and Nco1 and cloned in the forward orientation in pGL3-B. The resulting deletions have been designated here by the location of each 5’ end relative to the “A” (+1) in the translational start ATG for human XOR, and the clones designated phXD-B1 to phXD-B10, corresponding to 1,900bp and 200bp of upstream DNA respectively. A functional basal promoter was identified previously between +1 and −200bp and corresponds to phXDB10. This region has been extensively characterized [Xu et al., 1996]. Luciferase fusion constructs were confirmed by DNA sequence analysis as described [Wright et al., 2000]. All sequences were determined from both directions and sequence data were compiled manually. Oligonucleotides used as PCR or sequencing primers are available upon request.

XOR cDNA cloning and expression

Full length recombinant mouse XOR cDNA was obtained from Dr. Enrico Garattini (Mario Negri, Milan, Italy). Coding region sequence was amplified by PCR (PCR Extender System, 5-Prime, Inc, Broomfield, CO, USA) using the forward primer 5’-CATTTCCG**GTCGAC**CACGAGGACAACGGTAGATGAGTTG-3’ and the reverse primer 5’-GCCATTA**GCGGCCGC**GGAAACAGCTATGACCATGATTAC-3’. These primers were designed to create Sal I and Not I recognition sites, respectively (bold). The amplified sequence was cloned into the pCR2.1-TOPO vector (Invitrogen) using Sal I and Not I cleavage sites. The resulting clone was sequenced using M13 primers and the following internal forward primers: 5’-GTCATGAGTATGTACACACTGCTCCG-3’, 5’-GAGCAGAGGACAGAGGTGTTCAGAG-3’, 5’-CTGACAGTGCTTCAGAAGCTGGGC-3’, 5’-CACCTATGAAGACCTTCCAGCC-3’, and the internal reverse primers: 5’-CGAGAGAGATCCTCACTGTTCC-3’, 5’-GTACCTCCATGTGTCAGCAGCACC3’, 5’-GAGAGTAGTGCAGCTCCTCCATGG-3’, 5’-CTACGGTATGCACTTGACATTCCGAG-3’. DNA was excised from this clone with Sal I and Not I and cloned into the pCMV-Myc expression vector (Clontech) with the same restriction enzymes. This cloning strategy fuses in frame the amino terminal coding region of XOR with the cMyc tag encoded on pCMV-Myc. Recombinant DNA was prepared from *E. coli* TOP10 cells (Invitrogen) according to the manufacturer's recommendations. Clones were characterized by DNA sequencing using the pCMV forward primer 5’-GATCCGGTACTAGAGGAACTGAAAAAC-3’. The full length clone used in the present analysis has been designated pCMV-Myc-XOR-1 and has been referred to in the present communication as pCMVMyc-XOR.

Transfection and luciferase reporter assay

Cells to be transfected were grown to 70−80% of confluency in six well plates and shifted to 2 ml of fresh RPMI 1640 medium without serum or antibiotics one hour prior to transfection. Transfections were conducted using Lipofectamine 2000 (Invitrogen)

NIH-PA Author Manuscript

NIH-PA Author Manuscript

NIH-PA Author Manuscript

essentially as described by the supplier. Briefly, 5.1ug of total plasmid were mixed in 0.5ml of RPMI 1640 medium and subsequently mixed with 0.5ml of the same medium containing 10ul of Lipofectamine 2000. After combining both solutions and mixing, the transfecting solution was held at room temperature for 20 minutes and then applied to cells in one well of a six well plate. Medium was removed after 4hrs and replaced with standard growth medium. Cells were harvested for analysis after 48 hours of incubation. Cytoplasmic extracts were analysed for luciferase activity (Promega CCLR kit) using a BMG Lab Technologies (Durham, NC, USA) Lumistar luminometer. As reported by others, many β-galactosidase co-transfecting plasmids suppressed activity of the XOR reporter, including pRSV-β-galactosidase [Xu et al., 1996; Xu et al., 2000]. However, we observed that the co-transfecting plasmid pcDNA3.1(+)-HisMycLacZ exerted no suppressive effect on expression from any XOR deletion fusion. Thus, all transfections included 0.1ug of pcDNA3.1(+)-HisMycLacZ to normalize for transfection efficiency between cell lines. In addition, where plasmid titration was employed, pGEM4 was included at appropriate levels to bring the final mass of DNA to 5.1ug. β-galactosidase activity was determined exactly as described previously [Norton and Coffin, 1985]. Luciferase activity was normalized to both β-galactosidase units and to total cytoplasmic protein as determined spectrophotometrically using the bicinchoninic acid assay. Each individual transfection was assayed in quadruplicate, and each individual transfection was repeated six times, thus each value reported represents 24 biochemical assays for each parameter. Luciferase values represent arbitrary light units/mg protein/minute/β-galactosidase unit. Means and standard deviation were calculated for each group, and in most cases standard deviations were no greater than 10% of the mean value. Comparisons between groups used ANOVA or the Student's t-test where a p-value of <0.05 was considered significant.

HC11-C4 and HC11-C24 clonal selection

HC11-C4 and HC11-C24 were derived from the HC11 parental strain by limiting dilution. Single colonies were isolated, expanded, and tested for the development of F-actin stress fibers following treatment with recombinant mouse TGF-β1 (R&D Systems, Inc, Minnepolis, MN, USA). F-actin was detected using phalloidin staining. Time and dose response to TGF-β were optimized over a period of 0hr, 6hr, 12hr, days 1 through 9, and from 0 to 10 ng/ml of TGFβ, respectively. TGFβ was subsequently used at 5ng/ml with F-actin stress fibers analyzed over a 48hr time course. HC11-C4 and HC11-C24 were routinely maintained in RPMI 1640 medium containing 2.05 mM L-glutamine (Gibco) supplemented with 10% fetal bovine serum (FBS), 10ng/ml epidermal growth factor (EGF), 5μg/ml insulin, and 1X antibiotic antimycotic supplement (Gibco). When treated with TGF-β1, cells were switched to HI media (complete media containing heat inactivated FBS).

Immunofluorescent labeling

Six-well plates containing 22mm diameter cell culture treated coverslips (Nunc) were seeded at 1×10^5 cells/well and grown for two days. Cells were washed twice in ice cold PBS and fixed in 2% paraformaldehyde for fifteen minutes. The cells were rinsed with PBS and the aldehyde quenched with 0.1M glycine for five minutes. Cells were then incubated with Triton X-100 at 0.1% for 10 minutes. Non-specific protein binding was blocked with 1% BSA for 1 hour. F-actin was stained with Alexa Fluor 488 phalloidin (Invitrogen) by incubating cells for 15 minutes in a 1:100 dilution of the label in PBS. Cells were then washed, examined by fluorescent microscopy, and photographed.

Migration assay and Quantitation

The effect of XOR on migration of mouse and human MEC was determined as described [Dumont et al., 2003; Hayot et al., 2006; Steelant et al., 2002] except that cells were grown on 12 well plates and the monolayers wounded with a small bore plastic pipette tip.

NIH-PA Author Manuscript

NIH-PA Author Manuscript

NIH-PA Author Manuscript

Quantitation of migration was performed by open surface area calculation as described [Hayot et al., 2006]. Briefly, cells were photographed under constant magnification, the photographs printed at 260 × 175mm, and the remaining open surface area calculated. In setting the boundaries for surface area calculation lines were drawn on the leading edge of the cells such that as many cells fell to the left of the line as fell to the right of the line, as described [Hayot et al., 2006]. In all of the experiments shown here wounding was performed in triplicate and each wound was measured at three different points along the open wound. Thus, all quantitation was determined from nine independent measurements and the mean and standard deviation of the remaining open surface area are shown in each graph. Since the data shown here represent the remaining open surface area, an increase in migration appears as a decline in the remaining open surface area.

RESULTS

XOR activity is decreased in invasive MEC

The loss of XOR expression observed in clinically aggressive BC may reflect an unexpected property of the tumor, tissue handling, or a specific property of the tumor cells themselves. We examined levels of XOR activity in normal mouse (HC11), human (HB4a, MCF-10A), and cancerous (MCF-7, BT20, T47D, SBKR3, MDA-MB-231, MDA-MB-435) MEC. Consistent with clinical data derived from human mammary tumors [Linder et al., 2005], we observed high level XOR activity in normal mouse or human MEC, but markedly decreased XOR activity in human carcinoma cells (Fig. 1A). Similar levels of XOR activity were found in HC11, HB4a, and MCF-10A cells, while MCF-7, BT20, T47D, and SBKR3 cells exhibited levels of XOR activity that were intermediate between normal MEC and the highly aggressive MDA-MB-231 or MDA-MB-435 cells. Both XOR activity and protein level were very low in the highly invasive MDA-MB-231 human BC cell line, intermediate in MCF-7 cells, but high in HC11 and HB4a normal MEC (Fig. 1A, B).

XOR is poorly activated by post-confluent growth in invasive MEC

XOR exhibits post-confluent growth dependent induction in the HB4a normal human MEC [Page et al., 1998]. We quantitated MEC XOR activity (Fig. 2) and protein level over a 72 hour time course beginning from the point where cells had just reached 100% of confluence in standard growth medium. While all of the MEC studied exhibited post-confluent growth dependent induction of XOR, significant differences were also observed. Neither MCF-7 cells nor HB4a cells exhibited detectable XOR activity and very low protein levels initially (Fig. 2B, C). On the other hand, both HC11 and MDA-MB-231 cells exhibited detectable activity (Fig. 2A, D) and protein at the same point. Although induced by post-confluent growth in MDA-MB-231 cells, XOR activity and protein levels remained very low relative to all of the other cells studied (Fig. 2D).

XOR activity can be stimulated by NECA in highly invasive MDA-MB-231 cells

To determine whether the low level of XOR activity observed in MDA-MB-231 cells was the result of down-regulation *per se* or the result of a functionally deficient gene, we examined MDA-MB-231 cells for the capacity to induce XOR activity with n-ethylcarboxamido adenosine (NECA). NECA was previously found to be a potent inducer of XOR activity that may function through pathways known to activate XOR gene expression [Kelley et al., 2006]. As shown here (Fig. 2E), 48 hours of treatment with NECA induced XOR activity in both HC11 mouse MEC and in MDA-MB-231 cells. These data demonstrate that XOR activity can be induced in MDA-MB-231 cells and suggest that XOR expression may be down-regulated in MDA-MB-231 cells.

NIH-PA Author Manuscript

NIH-PA Author Manuscript

NIH-PA Author Manuscript

XOR promoter activation is decreased in invasive MEC

XOR is transcriptionally regulated in several different mammalian cells, including MEC [McManaman et al., 2000; Page et al., 1998; Seymour et al., 2006; Terada et al., 1997; Xu et al., 2000; Xu et al., 2004]. To determine if the XOR upstream regulatory DNA, including its previously characterized basal promoter [Martelin et al., 2000; Xu et al., 2000; Xu et al., 2004], was down-regulated in human MEC, 1,900bp of human XOR upstream DNA was cloned and fused in-frame with the translational start of the luciferase gene in the pGL3-Basic vector. Ten step-wise deletions of the XOR upstream DNA were generated. Transfection of each of these into HC11 mouse MEC or HB4a human MEC revealed a similar pattern of activation with the exception that the phXD-B10 DNA showed reduced expression in human MEC that was not observed in mouse MEC (Figs. 3A, B). Since phXD-B1 was comparably activated in both mouse and human cells, we transfected phXD-B1 into HC11 mouse MEC and into the human MECs HB4a, MCF-7, and MDA-MB-231 over a DNA titration range of 1, 2, 3, 4, and 5ug. While each cell showed increased luciferase expression with increasing DNA used in transfection (Fig. 3C), for each level of DNA used in transfection expression of the XOR upstream DNA was reduced in human cancer cells relative to that obtained in normal mouse or human MEC, in parallel with the data observed for XOR activity and protein level. These data confirm that XOR promoter activation is decreased in MCF-7 and MDA-MB-231 human mammary cancer cells.

XOR activity and protein level are decreased in clonally selected HC11 cells with high migratory activity

Our unpublished experiments had demonstrated that HC11 mouse MEC were heterogeneous with respect to their response to TGFβ stimulation and suggested that migratory activity in response to TGFβ may also be heterogeneous in HC11 cells as well. Single colonies were isolated from serially diluted cultures of HC11 and examined for the development of F-actin stress fibers in response to TGFβ. Two clones were isolated that differed dramatically in response to TGFβ, HC11-C4 and HC11-C24. HC11-C24 cells exhibited extensive F-actin stress fiber development after exposure to TGFβ whereas HC11-C4 exhibited markedly reduced response to TGFβ (Fig. 4A). We observed marked reduction in expression of α-smooth muscle actin (α-SMA) in response to TGFβ stimulation (Fig. 4B, C) when cells were examined over an extended time course. While both cells induced α-SMA transiently, and at the same point in time, HC11-C4 expressed approximately six fold less α-SMA expression at all time points. We tested HC11-C4 and HC11-C24 for migratory activity using a wounding assay in the presence or absence of TGFβ. Cells were examined 0, 19, and 31hrs after wounding and the addition of TGFβ. We observed that HC11-C24 showed extensive migration 31hrs after wounding whereas HC11-C4 exhibited markedly reduced migration in response to TGF-β throughout the 31hr time course (Fig. 4D, E). Significantly, HC11-C24 showed more extensive migration than HC-11-C4 even in the absence of TGFβ stimulation (Fig. 4D, E).

In parallel with the results obtained with the highly invasive human MDA-MB-231 cells, XOR activity and protein level in HC11-C24 were markedly reduced in contrast to HC11-C4 (Fig. 4F, G). A summary of several different characteristics of HC11-C4 and HC11-C24 is shown in Table 1. These data demonstrate that the reduced XOR activity and protein levels observed in the highly invasive MDA-MB-231 cells was paralleled in clonally selected HC11-C24 mouse MEC that also exhibit a high level of migratory activity *in vitro*.

Over-expression of XOR cDNA inhibits migratory activity of HC11-C24 and MDA-MB-231 cells

Recombinant mouse XOR cDNA was cloned into the expression vector pCMV-Myc to create pCMVMyc-XOR which was transfected into both HC11-C24 and MDA-MB-231

NIH-PA Author Manuscript

NIH-PA Author Manuscript

NIH-PA Author Manuscript

cells at different input doses of DNA. XOR activity was determined 24 hours later, and both mouse and human cells exhibited functional over-expression of the cDNA (Fig. 5A, B). Expression of Myc-tagged XOR in MDA-MB-231 was confirmed by western immunoblot against the Myc tag (Fig. 5C). HC11-C24 cells were transfected with pCMV-Myc-XOR or the empty vector in the presence or absence of the XOR specific inhibitor Y-700. After 24 hours, when the cells had reached confluency, they were subjected to wounding, quantitated, and representative photomicrographs obtained 0, 19, and 31hrs after wounding. Transfection with pCMVMyc-XOR, but not the empty vector, inhibited HC11-C24 migratory activity, and this effect was reversed by co-treatment with Y-700 (Fig. 5D, E). MDA-MB-231 cells were also transfected with pCMV-Myc-XOR or the empty vector in the presence or absence of Y-700 and the effect on wound induced migratory activity determined. As observed for HC11-C24 cells, MDA-MB-231 migratory activity was inhibited by over-expression of pCMV-Myc-XOR but not the empty vector (Fig. 5F, G). As observed with HC11-C24, co-treatment with Y-700 reversed the effect of pCMV-Myc-XOR on migratory activity. Thus, MEC of both mouse and human origin that exhibited markedly reduced XOR expression and a high degree of migratory activity showed reduced migration when induced to over-express XOR by transfection of recombinant XOR cDNA, and this effect was reversed by the XOR specific inhibitor Y-700.

Pharmacological inhibition of XOR stimulates migration in HC11-C4 and MCF-7 cells

HC11-C4 mouse or MCF-7 human MEC were grown to confluency and treated with either oxypurinol (150uM), allopurinol (150uM), Y-700 (1uM), or remained untreated. After one hour, cells were subjected to wounding, washed, and the medium refreshed in the presence of XOR inhibitors. The time course of migration was monitored in the absence of TGFβ stimulation. As shown in Figures 6A and 6B, all three XOR inhibitors quantitatively stimulated migration in HC11-C4 cells that was readily apparent 19hrs after wounding and was further stimulated 31hrs after wounding. Similar results were obtained for MCF-7 cells that were more marked 48hrs after wounding (Fig. 6C, D).

XOR derived ROS may contribute to suppression of MEC migration

HC11-C4 and MDA-MB-231 MEC, but not HC11-C24, both showed dose dependent activation of XOR by NECA (Fig. 7A). Accordingly, we exposed HC11-C4 and MDA-MB-231 to NECA over abroad concentration range in the absence or presence of either Y-700 or the ROS scavenger NAC. Cells were subjected to wounding which was quantitated 19hrs (HC11-C4) or 48hrs (MDA-MB-231) later. HC11-C4 exhibited a modest reduction in migratory rate by NECA treatment that was reversed by both Y-700 and NAC (Fig. 7B). MDA-MB-231 exhibited marked reduction in migratory rate by NECA which was also reversed by both Y-700 and NAC (Fig. 7C). To determine whether ROS scavenging in the absence of NECA would also affect MEC migratory rate, HC11-C4 and MDA-MB-231 were treated with NAC in the absence of NECA and migratory rate after wounding was determined. Both cells exhibited NAC dose dependent increase in migratory rate (Fig. 7D, E). The same experiment was performed in the presence of a broad concentration range of urate, a well recognized scavenger of both hydroxyl radical and peroxynitrite. Both HC11-C4 and MDA-MB-231 MEC exhibited urate dose dependent increase in migratory rate (Fig. 7F, G).

XOR modulates COX-2 expression in carcinoma and normal MEC

COX-2 may comprise a significant source of ROS in carcinoma and normal MEC [Smith et al., 2000], and its expression has been linked to invasiveness *in vivo* and migratory activity *in vitro* [Larkins et al., 2006; Singh et al., 2005]. We observed low or even decreasing expression of COX-2 with growth in MEC showing high XOR activity and weak migratory activity *in vitro* including HC11-C4, MCF-7, and HB4a (Fig. 8A). In contrast, HC11-C24

NIH-PA Author Manuscript

NIH-PA Author Manuscript

NIH-PA Author Manuscript

and MDA-MB-231 that exhibit low XOR activity and high migratory activity *in vitro* also exhibited high, growth induced levels of COX-2 (Fig. 8A). It was reported that heterozygous knockout of XOR in the germline revealed XOR to be an endogenous regulator of COX-2 in mouse fibroblasts, although these experiments did not report regulation in MEC [Ohtsubo et al., 2004]. Accordingly, we transfected the high COX-2 expressing HC11-C24 and MDA-MB-231 cells with pCMV-Myc-XOR or the control vector pCMV-Myc and examined COX-2 protein levels 48hrs later. We observed that forced ectopic over-expression of XOR reduced COX-2 expression in both cells (Fig. 8B). Conversely, treatment of HC11 and MCF-7 cells exhibiting high XOR and weak COX-2 protein levels with either oxypurinol or allopurinol resulted in increased levels of COX-2 protein (Fig. 8C). These data indicate that XOR also modulates COX-2 protein levels in both mouse and human MEC, and they suggest a potential mechanism by which XOR and COX-2 jointly contribute to migratory activity *in vitro*.

XOR modulates MMP1 and MMP3 levels and function in carcinoma MEC

Matrix metalloproteases play key roles in tumor metastasis, invasiveness, and MEC *in vitro* migratory activity [Brinckerhoff et al., 2000; Pei, 2005]. MMP1 and MMP3 specifically have been associated with increased MEC migratory activity *in vitro* [Davies et al., 1993; Pei, 2005; Wiesen and Werb, 1996]. We examined the effect of XOR inhibition on levels of MMP1 and MMP3 in MDA-MB-231 cells that had been cultured for 72hrs after reaching confluence where XOR exhibited low but significant induction. Both oxypurinol and Y-700 treatment increased levels of MMP1 and MMP3 (Fig. 9A) consistent with the increased migratory activity observed following Y-700 treatment of these cells. Treatment of MDA-MB-231 with NECA for 24hrs reduced expression of both COX-2 and MMP1, and Y-700 or NAC pretreatment blocked the decrease in COX-2 or MMP1 protein levels observed (Fig. 9B). To determine whether the suppressive role of XOR on MMP protein level was indeed reflected in the migratory activity of human carcinoma cells, we determine the effect of Y-700 in the presence or absence of MMP inhibitors I and III. We selected BT20 human mammary carcinoma cells for these analyses since they exhibited good but still intermediate levels of XOR activity (Fig. 1A). As shown in Fig. 9 (C, D), Y-700 alone stimulated BT20 migratory activity, and this effect was reversed by co-treatment with MMP inhibitors I and III. These data suggest that the suppressive role played by XOR on migratory activity *in vitro* may be mediated in part by reduction of COX-2 and MMP protein levels.

DISCUSSION

Clinical observations have suggested the possibility that down-regulation of XOR may be functionally linked to aggressive BC and BC recurrence. Consistent with these observations, data shown here revealed high levels of XOR activity and protein in normal mouse or human MEC that was reduced or markedly reduced in weakly or highly invasive human tumor cells, respectively. Investigation of the role of XOR expression on migration *in vitro* demonstrated that over-expression of recombinant XOR cDNA in the highly invasive MDA-MB-231 and in HC11-C24 cells that exhibit low XOR activity and protein levels inhibited migratory activity of both cells *in vitro*. Conversely, pharmacological inhibition of XOR in MCF-7 and HC11-C4 MEC that possess high levels of XOR activity and protein induced their migration *in vitro*. These data have revealed a functional link between XOR expression and the migration of MEC and suggest a potential role for the loss of XOR and the poor prognosis of BC patients expressing little or no XOR [Linder et al., 2005].

Data shown here have, for the first time, demonstrated that XOR activity, protein level, and promoter activation are decreased in human tumor derived MEC that exhibit highly invasive phenotype both *in vitro* and *in vivo*. MDA-MB-231 cells exhibit both high migratory activity *in vitro* [Larkins et al., 2006] and are highly invasive in mouse xenograft models *in vivo*

NIH-PA Author Manuscript

NIH-PA Author Manuscript

NIH-PA Author Manuscript

[Jiang et al., 2005; Li et al., 2007]. Importantly, MDA-MB-231 cells poorly expressed XOR and exhibited weak XOR promoter activation. That MDA-MB-231 cells exhibited strong XOR activation by NECA suggests that XOR was down-regulated in these cells and not functionally impaired. Our data also demonstrated that over-expression of recombinant XOR cDNA in MDA-MB-231 cells greatly reduced their migratory activity *in vitro*, and this identified a potential functional role for XOR in suppressing migratory activity. Similar observations were made in the clonally selected mouse MEC, HC11-C24. The HC11-C24 line was found to possess both low XOR activity and protein levels and high migratory activity *in vitro*, and over-expression of XOR cDNA in these cells also suppressed migratory activity. Thus, the capacity for XOR to suppress *in vitro* migration was independent of the species from which the MEC were derived, and it arose in cells with weak endogenous XOR expression.

The involvement of XOR in suppressing MEC migration was confirmed in the converse fashion using MCF-7 cells and the clonally selected HC11-C4 cells. MCF-7 cells exhibited intermediate levels of XOR activity, protein levels, and promoter activation that was higher than MDA-MB-231 but lower than HB4a normal human MEC. MCF-7 cells are weakly invasive *in vivo* [Aharinejad et al., 2004; Li et al., 2006] and exhibited weak migratory activity in the present *in vitro* experiments. Migratory activity of MCF-7 cells was significantly accelerated by three different XOR inhibitors: allopurinol, oxypurinol, and Y-700. The use of these different inhibitors is important because they possess very different capacity to scavenge ROS, and recent reports suggest that Y-700 may have no ROS scavenging capacity [Fukunari et al., 2004]. Furthermore, Y-700 exhibits very strong non-competitive inhibition of XOR with a reported K*i* of only 0.6nM [Fukunari et al., 2004]. Together, the three inhibitors unambiguously identify the contribution of XOR. Again, and in parallel with the previous experiments, the clonally selected HC11-C4 cell line provided further support for the contribution of XOR. HC11-C4 cells exhibited high levels of XOR activity and protein and weak migratory activity *in vitro* that was markedly accelerated by all three inhibitors. Thus, the contribution of XOR to suppression of MEC migration *in vitro* was demonstrated by the complementary action of XOR cDNA over-expression and the use of three very different pharmacological inhibitors of XOR.

While the mechanism by which XOR inhibits migratory activity is unknown, the capacity for XOR to contribute to functional differentiation [Anderson et al., 2007; Kurosaki et al., 1996; Linder et al., 1999; McManaman et al., 2000; McManaman et al., 1999; McManaman et al., 2002; Seymour et al., 2006] could in principal inhibit tumorigenesis or invasiveness, and by implication migration *in vitro*. However, as a source of intracellular ROS, RNS, or uric acid XOR may regulate many aspects of MEC function or signaling that could also modulate migratory activity. Stimulation of XOR activity with NECA reduced migratory rate in both HC11-C4 and MDA-MB-231 cells, and the XOR inhibitor Y-700 blocked NECA mediated inhibition of migration in both cell types. The involvement of ROS in the NECA response was demonstrated by co-treatment with N-acetylcysteine which resulted in marked increase in migratory activity of both cell types.

When the effect of ROS scavenging was tested in the absence of NECA activation an apparent paradox was uncovered. We tested the independent effects of NAC, a scavenger of hypochlorous acid (H--OCl), hydroxyl radical, and H2O2 [Aruoma et al., 1989], and urate, a scavenger of both peroxynitrite and hydroxyl radical. Both HC11-C4 (high XOR) and MDA-MB-231 (low XOR), showed markedly increased migratory activity in response to both NAC and urate. These data are readily reconciled for HC11-C4 by the high endogenous expression of XOR. The levels of urate used in these experiments (1.6 to 25 mg/dl) are commonly used in studies of ROS scavenging, however, it may be equally important that urate can also act to feedback inhibit XOR [Tan et al., 1993], and this may contribute to the

NIH-PA Author Manuscript

NIH-PA Author Manuscript

NIH-PA Author Manuscript

effects of urate on HC11-C4 migratory activity. In the case of MDA-MB-231 cells, however, the independent effects of NAC and urate suggest the presence of an additional source of ROS whose scavenging further increases migratory activity. It is paradoxical, then, that activation of XOR in MDA-MB-231 by NECA reduced migratory activity – an effect reversed by the XOR specific inhibitor Y-700. We imagine that activation of XOR in MDA-MB-231 cells may alter the global redox balance of the cells which then inhibits migratory activity. The complex reactions in which XOR may participate, including synthesis of urate, superoxide, or nitric oxide suggests many ways in which XOR could affect global redox balance, and further experiments will be needed to clarify this effect on migratory activity.

Previous reports demonstrated the key role of XOR in modulating COX-2 expression in mouse fibroblasts [Ohtsubo et al., 2004]. COX-2 is well recognized to promote tumorigenesis, metastasis, and migration [Liu et al., 2001; Lu et al., 2005; Singh et al., 2005], whereas its knockout or inhibition decreases tumorigenesis, migration, and invasiveness of mammary cancer cells [Howe et al., 2005; Larkins et al., 2006]. Our experiments uncovered a generally converse relation between XOR and COX-2. MEC exhibiting strong growth dependent expression of XOR (HC11-C4, HB4a, MCF-7) exhibited weak or declining COX-2 expression, while MEC exhibiting weak XOR expression showed high levels COX-2. Ectopic over-expression of XOR in these cells resulted in decreased COX-2 levels, and conversely inhibition of XOR in cells with strong expression increased levels of COX-2. Thus, XOR appears to modulate COX-2 protein levels in MEC of mouse or human origin. It is, however, important to note that expression of XOR does not preclude absolutely expression of COX-2. For example, in MDA-MB-231 cells COX-2 is vigorously induced by growth whereas XOR shows weak but positive induction at the same time. Nonetheless, over-expression of XOR both suppressed migratory activity *in vitro* and COX-2 protein levels.

The mechanisms underlying the converse, growth-dependent regulation of XOR and COX-2 are not understood. Growth-dependent effects on several aspects of MEC physiology, including XOR expression, have been studied [Fang et al., 2007; Page et al., 1998]. While growth-dependent transcriptional affects on XOR have been identified, the basis for these effects is also poorly understood. It was postulated that growth dependent resistance to antineoplastic drugs in MDA-MB-231 reflects contributions of both HIF-1 and unknown factors released by the cells [Fang et al., 2007]. We imagine that the forced ectopic over-expression of XOR could shift the intracellular redox balance in MEC and thereby modulate COX-2 expression. COX-2 appears to play a critical role in both migratory activity of mammary tumor cells [Rozic et al., 2001] and in promoting the survival of tumor cells [Lanza-Jacoby et al., 2006; Teh et al., 2004], and its modulation by XOR may both suppress migratory activity and compromise survival.

We observed a similar inverse relationship between XOR and levels of MMP1 and MMP3, and inhibition of XOR increased levels of both proteins in human carcinoma cells. MMPs are well recognized and important mediators of tumor cell migratory activity *in vitro* [Davies et al., 1993; Pei, 2005; Wiesen and Werb, 1996], and the increased levels of both MMP proteins observed by inhibition of XOR suggests that XOR suppresses either their maturation or protein expression. We postulated that if XOR suppressed MMP1 and MMP3, and MMPs were important mediators of carcinoma migratory activity *in vitro*, then inhibiting XOR with Y-700 would release MMPs from the inhibitory action of XOR and stimulate migratory activity. Furthermore, selective inhibition of MMP function in cells already inhibited for XOR activity should decrease migratory activity. We observed exactly this behavior in the human BT20 carcinoma cell line using two different MMP inhibitors. These data, therefore, provide strong corroborative evidence for the role of XOR in

NIH-PA Author Manuscript

NIH-PA Author Manuscript

NIH-PA Author Manuscript

decreasing *in vitro* migratory activity, a process mediated in part by the suppressive effect of XOR on MMP1 and MMP3 protein levels and function.

Our data suggest a mechanism that is consistent with both the observed effects on migratory activity *in vitro*, XOR and COX-2 expression, and recent clinical observations (Fig. 10). We imagine that in cells showing high XOR expression (Fig. 10) that it, and additional but unknown factors, contribute to modulation of COX-2 and the subsequent down regulation of COX-2 derived ROS, leading to dampening of MMP expression, migratory activity, and an improved clinical outcome. COX-2 is well known to generate superoxide which can be reduced to hydrogen peroxide, a potential mediator of MMP expression [Zhang et al., 2002] that stimulates tumor progression and migratory activity [Storz, 2005;Wu, 2006]. In the converse situation, where COX-2 is highly expressed and XOR poorly expressed, COX-2 may contribute significantly to MMP expression, migratory activity, and poor clinical outcome. NAC and urate may stimulate migratory activity *in vitro* as scavengers of ROS/RNS derived from other unknown sources and perhaps in part from XOR. The capacity for XOR to reduce levels of COX-2, MMPs, and migratory activity has great significance for modulating the course of BC progression and metastasis. Identifying the mechanisms that underlie this process may offer unique opportunities for chemoprevention or novel intervention not previously investigated for BC.

Acknowledgments

The authors would like to thank Dr. Enrico Garattini (Mario Negri, Milan, Italy) for the recombinant mouse XOR cDNA and Dr. Atushi Fukunari (Mitsubishi Tanabe Pharma Corporation, Yokohama, Japan) for the XOR inhibitor, Y-700. This work was supported by the generosity of the Robert and Helen Kleberg Foundation, the American Cancer Society (PF-06−005−01−CCE, PF-08−112−01-CCE), and by the National Institutes of Health (RO1-HL045582).

REFERENCES

Aharinejad S, Paulus P, Sioud M, Hofmann M, Zins K, Schafer R, Stanley ER, Abraham D. Colony-stimulating factor-1 blockade by antisense oligonucleotides and small interfering RNAs suppresses growth of human mammary tumor xenografts in mice. Cancer Res. 2004; 64:5378–84. [PubMed: 15289345]

Alsabti E. Serum xanthine oxidase in breast carcinoma. Neoplasma. 1980; 27:95–9. [PubMed: 6892840]

Anderson SM, Rudolph MC, McManaman JL, Neville MC. Key stages in mammary gland development. Secretory activation in the mammary gland: it's not just about milk protein synthesis! Breast Cancer Res. 2007; 9:204. [PubMed: 17338830]

Aruoma OI, Halliwell B, Hoey BM, Butler J. The antioxidant action of N-acetylcysteine: its reaction with hydrogen peroxide, hydroxyl radical, superoxide, and hypochlorous acid. Free Radic Biol Med. 1989; 6:593–7. [PubMed: 2546864]

Becker BF. Towards the physiological function of uric acid. Free Radic Biol Med. 1993; 14:615–31. [PubMed: 8325534]

Brinckerhoff CE, Rutter JL, Benbow U. Interstitial collagenases as markers of tumor progression. Clin Cancer Res. 2000; 6:4823–30. [PubMed: 11156241]

Castro GD, Layno AM, Fanelli SL, Maciel ME, Gomez MI, Castro JA. Acetaldehyde accumulation in rat mammary tissue after an acute treatment with alcohol. J Appl Toxicol. 2007

Cheung KJ, Tzameli I, Pissios P, Rovira I, Gavrilova O, Ohtsubo T, Chen Z, Finkel T, Flier JS, Friedman JM. Xanthine oxidoreductase is a regulator of adipogenesis and PPARgamma activity. Cell Metab. 2007; 5:115–28. [PubMed: 17276354]

Clark MP, Chow CW, Rinaldo JE, Chalkley R. Correct usage of multiple transcription initiation sites and C/EBP-dependent transcription activation of the rat XDH/XO TATA-less promoter requires downstream elements located in the coding region of the gene. Nucleic Acids Res. 1998a; 26:1801–6. [PubMed: 9512555]

NIH-PA Author Manuscript NIH-PA Author Manuscript NIH-PA Author Manuscript

Clark MP, Chow CW, Rinaldo JE, Chalkley R. Multiple domains for initiator binding proteins TFII-I and YY-1 are present in the initiator and upstream regions of the rat XDH/XO TATA-less promoter. Nucleic Acids Res. 1998b; 26:2813–20. [PubMed: 9592172]

Cook WS, Chu R, Saksela M, Raivio KO, Yelandi AV. Differential immunohistochemical localization of xanthine oxidase in normal and neoplastic human breast epithelium. Int J Oncol. 1997; 11:1013–1017. [PubMed: 21528298]

Davies B, Miles DW, Happerfield LC, Naylor MS, Bobrow LG, Rubens RD, Balkwill FR. Activity of type IV collagenases in benign and malignant breast disease. Br J Cancer. 1993; 67:1126–31. [PubMed: 8494711]

Dumont N, Bakin AV, Arteaga CL. Autocrine transforming growth factor-beta signaling mediates Smad-independent motility in human cancer cells. J Biol Chem. 2003; 278:3275–85. [PubMed: 12421823]

Fang Y, Sullivan R, Graham CH. Confluence-dependent resistance to doxorubicin in human MDA-MB-231 breast carcinoma cells requires hypoxia-inducible factor-1 activity. Exp Cell Res. 2007; 313:867–77. [PubMed: 17289019]

Fukunari A, Okamoto K, Nishino T, Eger BT, Pai EF, Kamezawa M, Yamada I, Kato N. Y-700 [1-[3-Cyano-4-(2,2-dimethylpropoxy)phenyl]-1H-pyrazole-4-carboxylic acid]: a potent xanthine oxidoreductase inhibitor with hepatic excretion. J Pharmacol Exp Ther. 2004; 311:519–28. [PubMed: 15190124]

Garattini E, Mendel R, Romao MJ, Wright R, Terao M. Mammalian molybdo-flavoenzymes, an expanding family of proteins: structure, genetics, regulation, function and pathophysiology. Biochem J. 2003; 372:15–32. [PubMed: 12578558]

Godber BL, Doel JJ, Sapkota GP, Blake DR, Stevens CR, Eisenthal R, Harrison R. Reduction of nitrite to nitric oxide catalyzed by xanthine oxidoreductase. J Biol Chem. 2000; 275:7757–63. [PubMed: 10713088]

Griguer CE, Oliva CR, Kelley EE, Giles GI, Lancaster JR Jr. Gillespie GY. Xanthine oxidase-dependent regulation of hypoxia-inducible factor in cancer cells. Cancer Res. 2006; 66:2257–63. [PubMed: 16489029]

Hayot C, Debeir O, Van Ham P, Van Damme M, Kiss R, Decaestecker C. Characterization of the activities of actin-affecting drugs on tumor cell migration. Toxicol Appl Pharmacol. 2006; 211:30–40. [PubMed: 16005926]

Hooper DC, Scott GS, Zborek A, Mikheeva T, Kean RB, Koprowski H, Spitsin SV. Uric acid, a peroxynitrite scavenger, inhibits CNS inflammation, blood-CNS barrier permeability changes, and tissue damage in a mouse model of multiple sclerosis. Faseb J. 2000; 14:691–8. [PubMed: 10744626]

Howe LR, Chang SH, Tolle KC, Dillon R, Young LJ, Cardiff RD, Newman RA, Yang P, Thaler HT, Muller WJ, Hudis C, Brown AM, Hla T, Subbaramaiah K, Dannenberg AJ. HER2/neu-induced mammary tumorigenesis and angiogenesis are reduced in cyclooxygenase-2 knockout mice. Cancer Res. 2005; 65:10113–9. [PubMed: 16267038]

Hynes NE, Taverna D, Harwerth IM, Ciardiello F, Salomon DS, Yamamoto T, Groner B. Epidermal growth factor receptor, but not c-erbB-2, activation prevents lactogenic hormone induction of the beta-casein gene in mouse mammary epithelial cells. Mol Cell Biol. 1990; 10:4027–34. [PubMed: 2196443]

Jiang WG, Davies G, Martin TA, Parr C, Watkins G, Mason MD, Mokbel K, Mansel RE. Targeting matrilysin and its impact on tumor growth in vivo: the potential implications in breast cancer therapy. Clin Cancer Res. 2005; 11:6012–9. [PubMed: 16115946]

Kean RB, Spitsin SV, Mikheeva T, Scott GS, Hooper DC. The peroxynitrite scavenger uric acid prevents inflammatory cell invasion into the central nervous system in experimental allergic encephalomyelitis through maintenance of blood-central nervous system barrier integrity. J Immunol. 2000; 165:6511–8. [PubMed: 11086092]

Kelley EE, Hock T, Khoo NK, Richardson GR, Johnson KK, Powell PC, Giles GI, Agarwal A, Lancaster JR Jr. Tarpey MM. Moderate hypoxia induces xanthine oxidoreductase activity in arterial endothelial cells. Free Radic Biol Med. 2006; 40:952–9. [PubMed: 16540390]

NIH-PA Author Manuscript NIH-PA Author Manuscript NIH-PA Author Manuscript

Kurosaki M, Zanotta S, Li Calzi M, Garattini E, Terao M. Expression of xanthine oxidoreductase in mouse mammary epithelium during pregnancy and lactation: regulation of gene expression by glucocorticoids and prolactin. Biochem J. 1996; 319(Pt 3):801–10. [PubMed: 8920983]

Lanza-Jacoby S, Burd R, Rosato FE Jr. McGuire K, Little J, Nougbilly N, Miller S. Effect of simultaneous inhibition of epidermal growth factor receptor and cyclooxygenase-2 in HER-2/neupositive breast cancer. Clin Cancer Res. 2006; 12:6161–9. [PubMed: 17062693]

Larkins TL, Nowell M, Singh S, Sanford GL. Inhibition of cyclooxygenase-2 decreases breast cancer cell motility, invasion and matrix metalloproteinase expression. BMC Cancer. 2006; 6:181. [PubMed: 16831226]

Lewin I, Lewin R, Bray RC. Xanthine oxidase activity during mammary carcinogenesis in mice. Nature. 1957; 180:763–4. [PubMed: 13477276]

Li H, Samouilov A, Liu X, Zweier JL. Characterization of the effects of oxygen on xanthine oxidase-mediated nitric oxide formation. J Biol Chem. 2004; 279:16939–46. [PubMed: 14766900]

Li W, Hardwick MJ, Rosenthal D, Culty M, Papadopoulos V. Peripheral-type benzodiazepine receptor overexpression and knockdown in human breast cancer cells indicate its prominent role in tumor cell proliferation. Biochem Pharmacol. 2007; 73:491–503. [PubMed: 17126818]

Li ZB, Zeng ZJ, Chen Q, Luo SQ, Hu WX. Recombinant AAV-mediated HSVtk gene transfer with direct intratumoral injections and Tet-On regulation for implanted human breast cancer. BMC Cancer. 2006; 6:66. [PubMed: 16539746]

Linder N, Haglund C, Lundin M, Nordling S, Ristimaki A, Kokkola A, Mrena J, Wiksten JP, Lundin J. Decreased xanthine oxidoreductase is a predictor of poor prognosis in early-stage gastric cancer. J Clin Pathol. 2006; 59:965–71. [PubMed: 16935971]

Linder N, Lundin J, Isola J, Lundin M, Raivio KO, Joensuu H. Down-regulated xanthine oxidoreductase is a feature of aggressive breast cancer. Clin Cancer Res. 2005; 11:4372–81. [PubMed: 15958620]

Linder N, Rapola J, Raivio KO. Cellular expression of xanthine oxidoreductase protein in normal human tissues. Lab Invest. 1999; 79:967–74. [PubMed: 10462034]

Liu CH, Chang SH, Narko K, Trifan OC, Wu MT, Smith E, Haudenschild C, Lane TF, Hla T. Overexpression of cyclooxygenase-2 is sufficient to induce tumorigenesis in transgenic mice. J Biol Chem. 2001; 276:18563–9. [PubMed: 11278747]

Lo IC, Shih JM, Jiang MJ. Reactive oxygen species and ERK 1/2 mediate monocyte chemotactic protein-1-stimulated smooth muscle cell migration. J Biomed Sci. 2005; 12:377–88. [PubMed: 15917991]

Lu S, Yu G, Zhu Y, Archer MC. Cyclooxygenase-2 overexpression in MCF-10F human breast epithelial cells inhibits proliferation, apoptosis and differentiation, and causes partial transformation. Int J Cancer. 2005; 116:847–52. [PubMed: 15856465]

Maciel ME, Castro GD, Castro JA. Inhibition of the rat breast cytosolic bioactivation of ethanol to acetaldehyde by some plant polyphenols and folic acid. Nutr Cancer. 2004; 49:94–9. [PubMed: 15456641]

Maia L, Duarte RO, Ponces-Freire A, Moura JJ, Mira L. NADH oxidase activity of rat and human liver xanthine oxidoreductase: potential role in superoxide production. J Biol Inorg Chem. 2007; 12:777–87. [PubMed: 17440754]

Maia L, Vala A, Mira L. NADH oxidase activity of rat liver xanthine dehydrogenase and xanthine oxidase-contribution for damage mechanisms. Free Radic Res. 2005; 39:979–86. [PubMed: 16087479]

Martelin E, Palvimo JJ, Lapatto R, Raivio KO. Nuclear factor Y activates the human xanthine oxidoreductase gene promoter. FEBS Lett. 2000; 480:84–8. [PubMed: 11034305]

Matuschak GM, Lechner AJ, Chen Z, Todi S, Doyle TM, Loftis LL. Hypoxic suppression of E. coli-induced NF-kappa B and AP-1 transactivation by oxyradical signaling. Am J Physiol Regul Integr Comp Physiol. 2004; 287:R437–45. [PubMed: 15059791]

McManaman JL, Hanson L, Neville MC, Wright RM. Lactogenic hormones regulate xanthine oxidoreductase and beta-casein levels in mammary epithelial cells by distinct mechanisms. Arch Biochem Biophys. 2000; 373:318–27. [PubMed: 10620355]

NIH-PA Author Manuscript NIH-PA Author Manuscript NIH-PA Author Manuscript

McManaman JL, Neville MC, Wright RM. Mouse mammary gland xanthine oxidoreductase: purification, characterization, and regulation. Arch Biochem Biophys. 1999; 371:308–16. [PubMed: 10545219]

McManaman JL, Palmer CA, Wright RM, Neville MC. Functional regulation of xanthine oxidoreductase expression and localization in the mouse mammary gland: evidence of a role in lipid secretion. J Physiol. 2002; 545:567–79. [PubMed: 12456835]

Millar TM. Peroxynitrite formation from the simultaneous reduction of nitrite and oxygen by xanthine oxidase. FEBS Lett. 2004; 562:129–33. [PubMed: 15044013]

Norton PA, Coffin JM. Bacterial beta-galactosidase as a marker of Rous sarcoma virus gene expression and replication. Mol Cell Biol. 1985; 5:281–90. [PubMed: 2983187]

Ohtsubo T, Rovira II, Starost MF, Liu C, Finkel T. Xanthine oxidoreductase is an endogenous regulator of cyclooxygenase-2. Circ Res. 2004; 95:1118–24. [PubMed: 15528468]

Page S, Powell D, Benboubetra M, Stevens CR, Blake DR, Selase F, Wolstenholme AJ, Harrison R. Xanthine oxidoreductase in human mammary epithelial cells: activation in response to inflammatory cytokines. Biochim Biophys Acta. 1998; 1381:191–202. [PubMed: 9685639]

Pei D. Matrix metalloproteinases target protease-activated receptors on the tumor cell surface. Cancer Cell. 2005; 7:207–8. [PubMed: 15766657]

Roberts LE, Fini MA, Derkash N, Wright RM. PD98059 enhanced insulin, cytokine, and growth factor activation of xanthine oxidoreductase in epithelial cells involves STAT3 and the glucocorticoid receptor. J Cell Biochem. 2007; 101:1567–87. [PubMed: 17370312]

Rozic JG, Chakraborty C, Lala PK. Cyclooxygenase inhibitors retard murine mammary tumor progression by reducing tumor cell migration, invasiveness and angiogenesis. Int J Cancer. 2001; 93:497–506. [PubMed: 11477553]

Sanders SA, Eisenthal R, Harrison R. NADH oxidase activity of human xanthine oxidoreductase--generation of superoxide anion. Eur J Biochem. 1997; 245:541–8. [PubMed: 9182988]

Seymour KJ, Roberts LE, Fini MA, Parmley LA, Oustitch TL, Wright RM. Stress activation of mammary epithelial cell xanthine oxidoreductase is mediated by p38 MAPK and CCAAT/enhancer-binding protein-beta. J Biol Chem. 2006; 281:8545–58. [PubMed: 16452486]

Shan L, He M, Yu M, Qiu C, Lee NH, Liu ET, Snyderwine EG. cDNA microarray profiling of rat mammary gland carcinomas induced by 2-amino-1-methyl-6-phenylimidazo[4,5-b]pyridine and 7,12-dimethylbenz[a]anthracene. Carcinogenesis. 2002; 23:1561–8. [PubMed: 12376462]

Shim H, Shim E, Lee H, Hahn J, Kang D, Lee YS, Jeoung D. CAGE, a novel cancer/testis antigen gene, promotes cell motility by activation ERK and p38 MAPK and downregulating ROS. Mol Cells. 2006; 21:367–75. [PubMed: 16819299]

Singh B, Berry JA, Shoher A, Ramakrishnan V, Lucci A. COX-2 overexpression increases motility and invasion of breast cancer cells. Int J Oncol. 2005; 26:1393–9. [PubMed: 15809733]

Smith WL, DeWitt DL, Garavito RM. Cyclooxygenases: structural, cellular, and molecular biology. Annu Rev Biochem. 2000; 69:145–82. [PubMed: 10966456]

Steelant WF, Kawakami Y, Ito A, Handa K, Bruyneel EA, Mareel M, Hakomori S. Monosialyl-Gb5 organized with cSrc and FAK in GEM of human breast carcinoma MCF-7 cells defines their invasive properties. FEBS Lett. 2002; 531:93–8. [PubMed: 12401210]

Storz P. Reactive oxygen species in tumor progression. Front Biosci. 2005; 10:1881–96. [PubMed: 15769673]

Tan S, Radi R, Gaudier F, Evans RA, Rivera A, Kirk KA, Parks DA. Physiologic levels of uric acid inhibit xanthine oxidase in human plasma. Pediatr Res. 1993; 34:303–7. [PubMed: 8134172]

Teh SH, Hill AK, Foley DA, McDermott EW, O'Higgins NJ, Young LS. COX inhibitors modulate bFGF-induced cell survival in MCF-7 breast cancer cells. J Cell Biochem. 2004; 91:796–807. [PubMed: 14991771]

Terada LS, Piermattei D, Shibao GN, McManaman JL, Wright RM. Hypoxia regulates xanthine dehydrogenase activity at pre- and posttranslational levels. Arch Biochem Biophys. 1997; 348:163–8. [PubMed: 9390187]

Vorbach C, Scriven A, Capecchi MR. The housekeeping gene xanthine oxidoreductase is necessary for milk fat droplet enveloping and secretion: gene sharing in the lactating mammary gland. Genes Dev. 2002; 16:3223–35. [PubMed: 12502743]

NIH-PA Author Manuscript

NIH-PA Author Manuscript

NIH-PA Author Manuscript

Wiesen JF, Werb Z. The role of stromelysin-1 in stromal-epithelial interactions and cancer. Enzyme Protein. 1996; 49:174–81. [PubMed: 8797005]

Wright RM, McManaman JL, Repine JE. Alcohol-induced breast cancer: a proposed mechanism. Free Radic Biol Med. 1999; 26:348–54. [PubMed: 9895226]

Wright RM, Riley MG, Weigel LK, Ginger LA, Costantino DA, McManaman JL. Activation of the human aldehyde oxidase (hAOX1) promoter by tandem cooperative Sp1/Sp3 binding sites: identification of complex architecture in the hAOX upstream DNA that includes a proximal promoter, distal activation sites, and a silencer element. DNA Cell Biol. 2000; 19:459–74. [PubMed: 10975464]

Wu WS. The signaling mechanism of ROS in tumor progression. Cancer Metastasis Rev. 2006; 25:695–705. [PubMed: 17160708]

Wu WS, Tsai RK, Chang CH, Wang S, Wu JR, Chang YX. Reactive oxygen species mediated sustained activation of protein kinase C alpha and extracellular signal-regulated kinase for migration of human hepatoma cell Hepg2. Mol Cancer Res. 2006; 4:747–58. [PubMed: 17050668]

Xu P, Huecksteadt TP, Hoidal JR. Molecular cloning and characterization of the human xanthine dehydrogenase gene (XDH). Genomics. 1996; 34:173–80. [PubMed: 8661045]

Xu P, LaVallee P, Hoidal JR. Repressed expression of the human xanthine oxidoreductase gene. E-box and TATA-like elements restrict ground state transcriptional activity. J Biol Chem. 2000; 275:5918–26. [PubMed: 10681584]

Xu P, LaVallee PA, Lin JJ, Hoidal JR. Characterization of proteins binding to E-box/Ku86 sites and function of Ku86 in transcriptional regulation of the human xanthine oxidoreductase gene. J Biol Chem. 2004; 279:16057–63. [PubMed: 14761964]

Zhang HJ, Zhao W, Venkataraman S, Robbins ME, Buettner GR, Kregel KC, Oberley LW. Activation of matrix metalloproteinase-2 by overexpression of manganese superoxide dismutase in human breast cancer MCF-7 cells involves reactive oxygen species. J Biol Chem. 2002; 277:20919–26. [PubMed: 11929863]

NIH-PA Author Manuscript

NIH-PA Author Manuscript

NIH-PA Author Manuscript

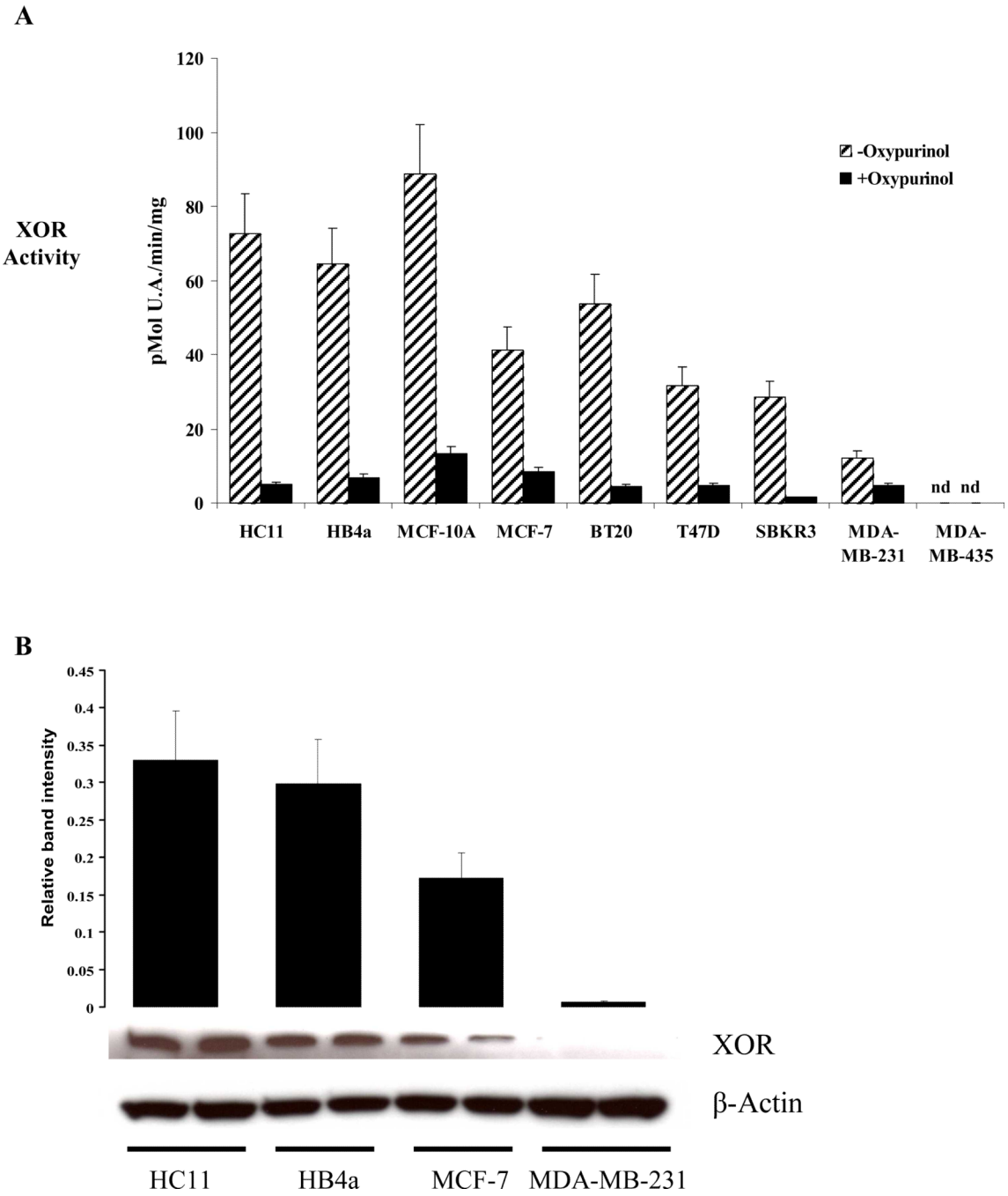

FIGURE 1. Expression of XOR activity and protein level in normal mouse and human MEC and in human BC cells

A, the cells indicated were grown for five days after plating in standard rich medium. Cells were harvested, extracts prepared, and total XOR activity was determined by spectroscopic assay of uric acid formation. Data are pMoles of uric acid/min/mg of protein. The mean and SD of six determinations (hatched bars) are shown. Oxypurinol was included in separate reactions at 150uM to confirm specificity (black bars) of urate generation. *B*, XOR protein level was determined from duplicate samples of four selected cells by western immunoblot, and β-Actin expression was used to control for loading of the gels.

NIH-PA Author Manuscript

NIH-PA Author Manuscript

NIH-PA Author Manuscript

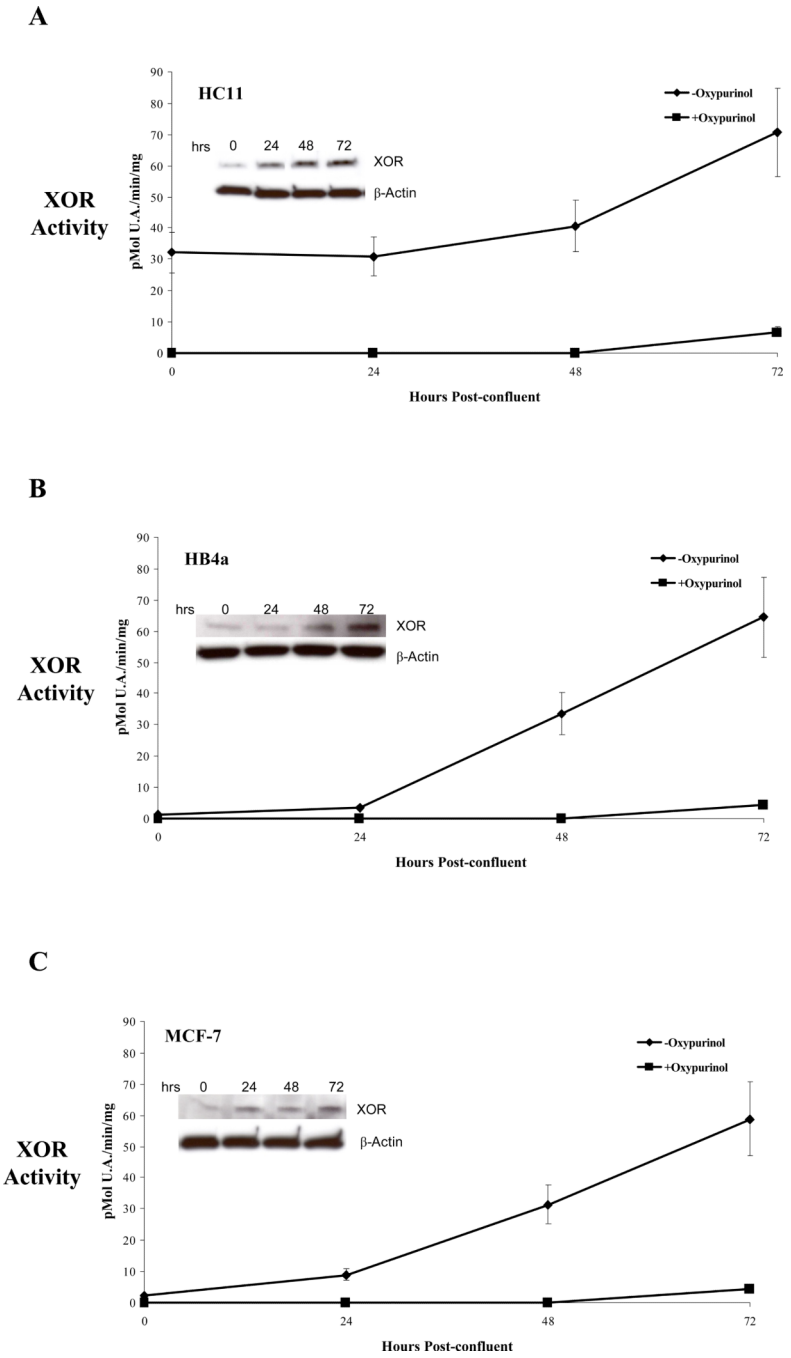

NIH-PA Author Manuscript

NIH-PA Author Manuscript

NIH-PA Author Manuscript

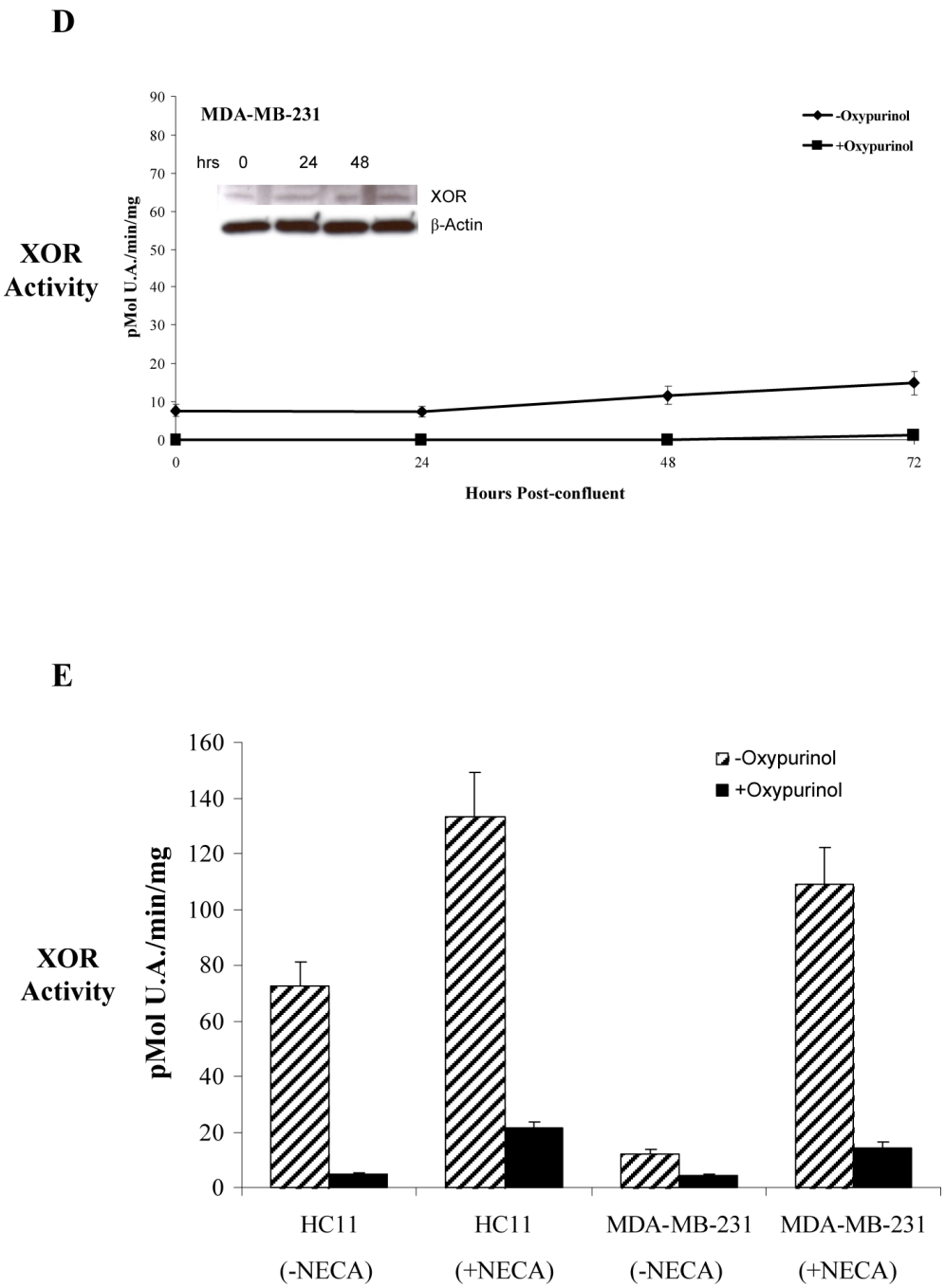

FIGURE 2. Post-confluent induction of XOR activity in mouse and human MEC

The indicated cells were grown to confluency and cells were harvested then and every 24hrs for three days (0, 24, 48, and 72hrs post-confluent). XOR activity was determined from whole cell extracts, and data show the mean and standard deviation of six determinations at each time point. Western immunoblots were run for each of the cells, blots were repeated three times, and representative blots are shown for each cell and included as inset photopgraphs. *A*, HC11 mouse MEC; *B*, HB4a human MEC; *C*, MCF-7 human carcinoma; *D*, MDA-MB-231 human carcinoma. *D*, NECA activation of XOR in HC11 and MDA-MB-231 cells. HC11 and MDA-MB-231 cells were grown to confluency in six well trays,

treated with 50uM NECA, and XOR activity was determined from whole cells extracts 48 hours later. Data show the mean and standard deviation of six independent determinations.

NIH-PA Author Manuscript

NIH-PA Author Manuscript

NIH-PA Author Manuscript

NIH-PA Author Manuscript

NIH-PA Author Manuscript

NIH-PA Author Manuscript

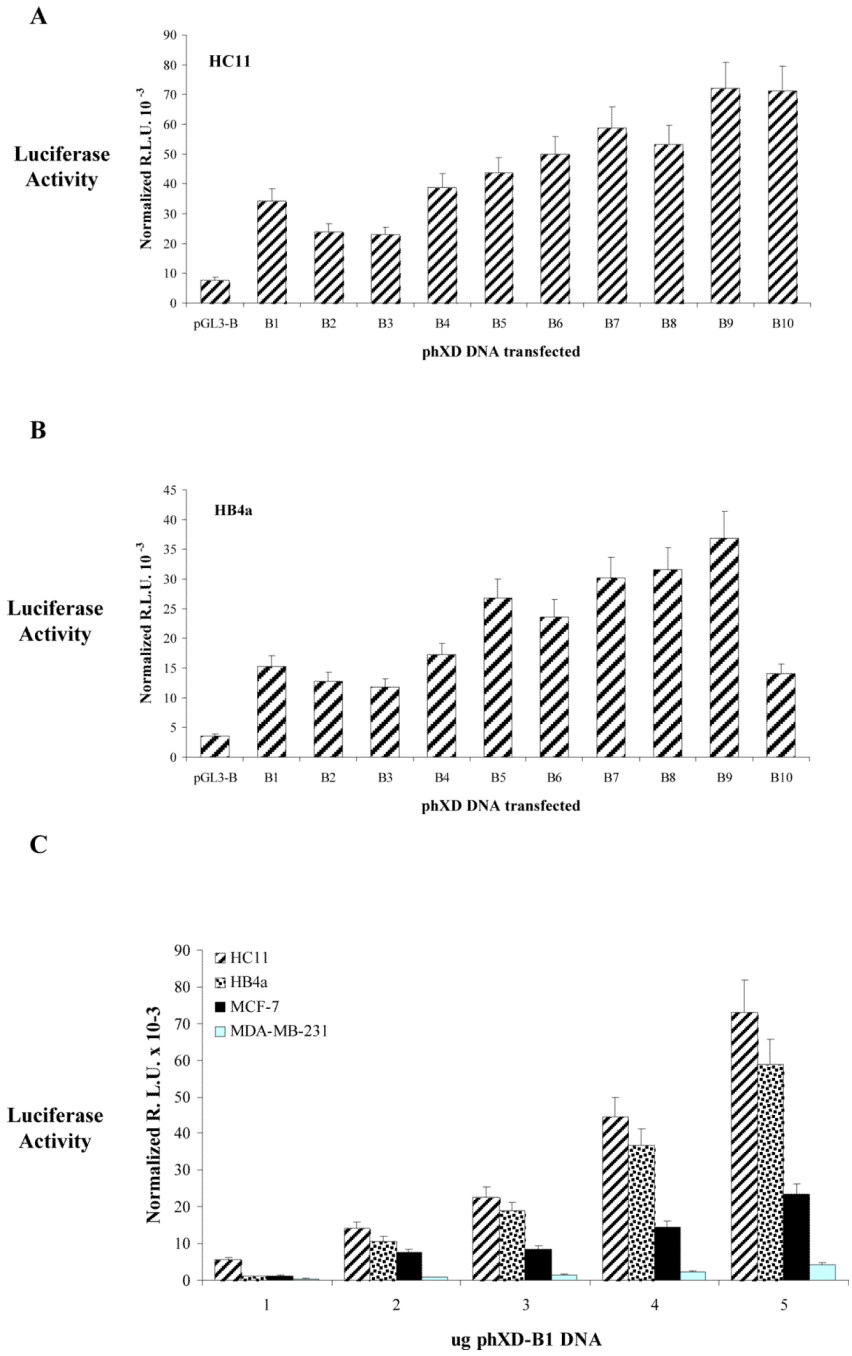

FIGURE 3. Activation of the human XOR promoter and upstream regulatory DNA in normal mouse and human MEC and in human BC cells

A, *B*, ten individual clones of the XOR deletion set, spanning the upstream region from −1,900bp to −200bp, were transfected into mouse HC11 or human HB4a MEC respectively. Expression from each deletion was determined 48hrs after transfection. The parent expression vector, pGL3-Basic (pGL3-B) was transfected independently in each series. Note, the B10 designation, for example, corresponds to phXD-B10 and comprises the previously characterized XOR promoter, while B1 corresponds to phXD-B1 and comprises 1.9kbp of upstream regulatory DNA. *C*, the phXD-B1 clone containing 1.9kbp of XOR upstream regulatory DNA, including the proximal 200bp promoter, was transfected into the

NIH-PA Author Manuscript

NIH-PA Author Manuscript

NIH-PA Author Manuscript

indicated cells at 1.0 to 5.0ug of DNA. Cells were co-transfected with 0.1ug of pcDNA3.1(+)HisMycLacZ and sufficient amounts of pGEM4 to bring the total mass of DNA to 5.1ug. Cells were harvested after 48hrs, and luciferase expression and lacZ expression were determined. Data were normalized to the amount of lacZ expression and are shown as normalized relative light units (R.L.U.).

NIH-PA Author Manuscript

NIH-PA Author Manuscript

NIH-PA Author Manuscript

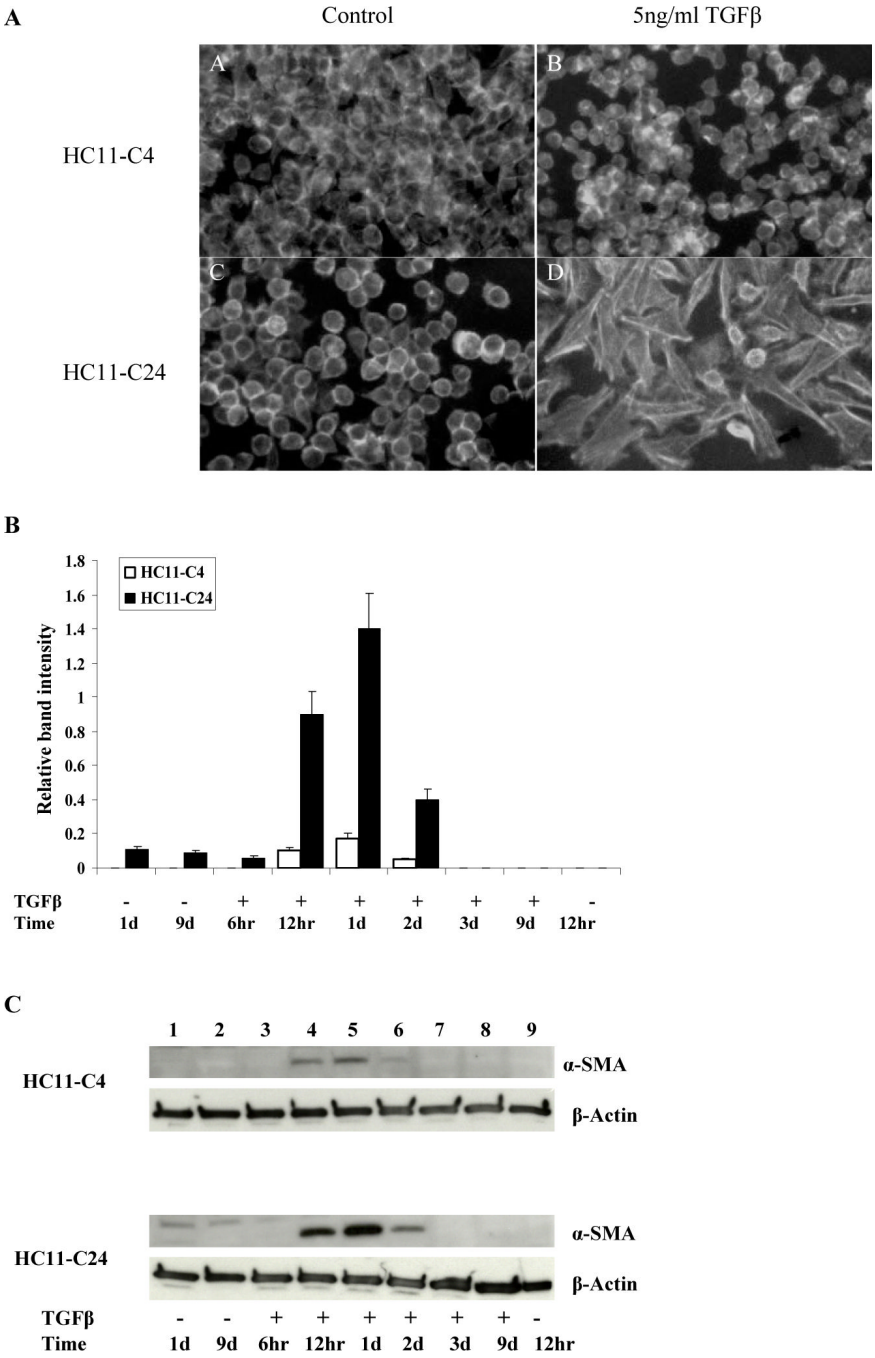

NIH-PA Author Manuscript

NIH-PA Author Manuscript

NIH-PA Author Manuscript

D

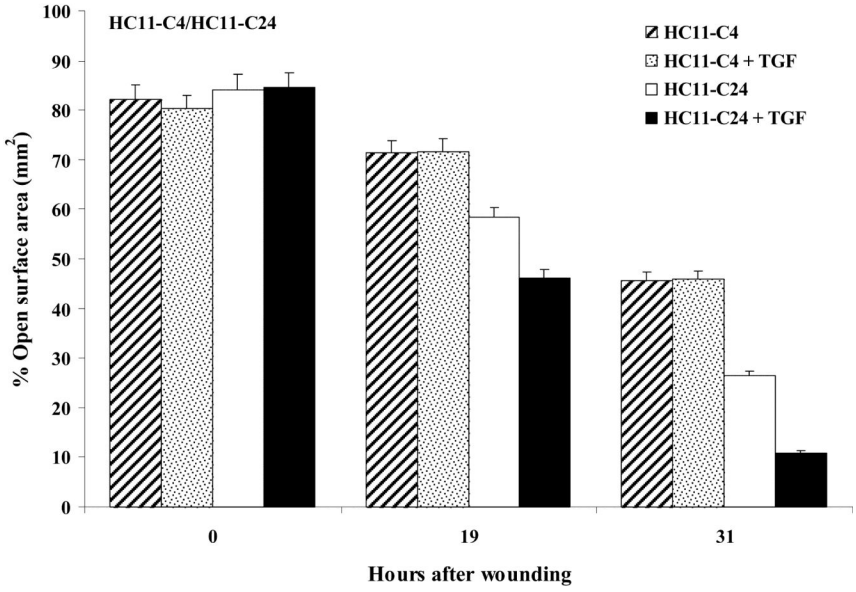

E

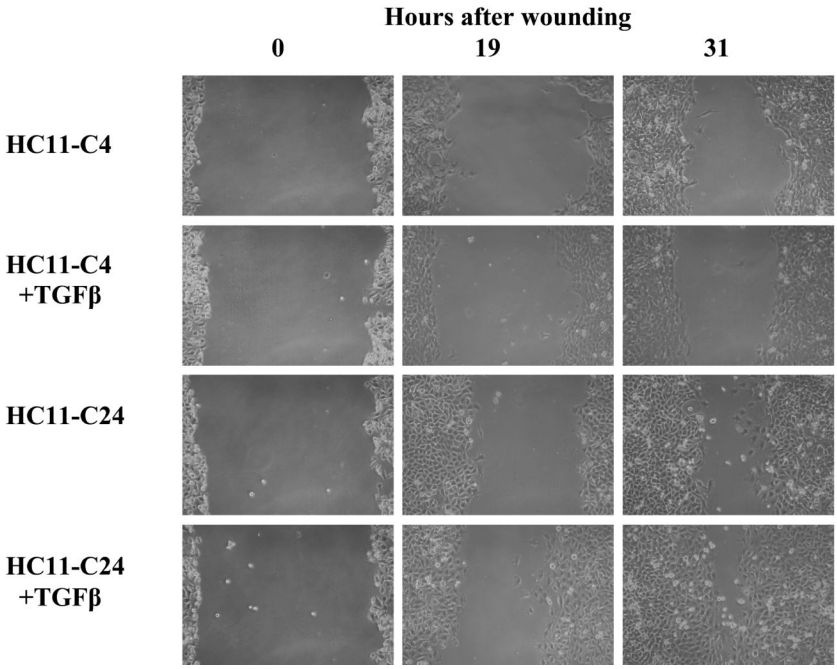

NIH-PA Author Manuscript

NIH-PA Author Manuscript

NIH-PA Author Manuscript

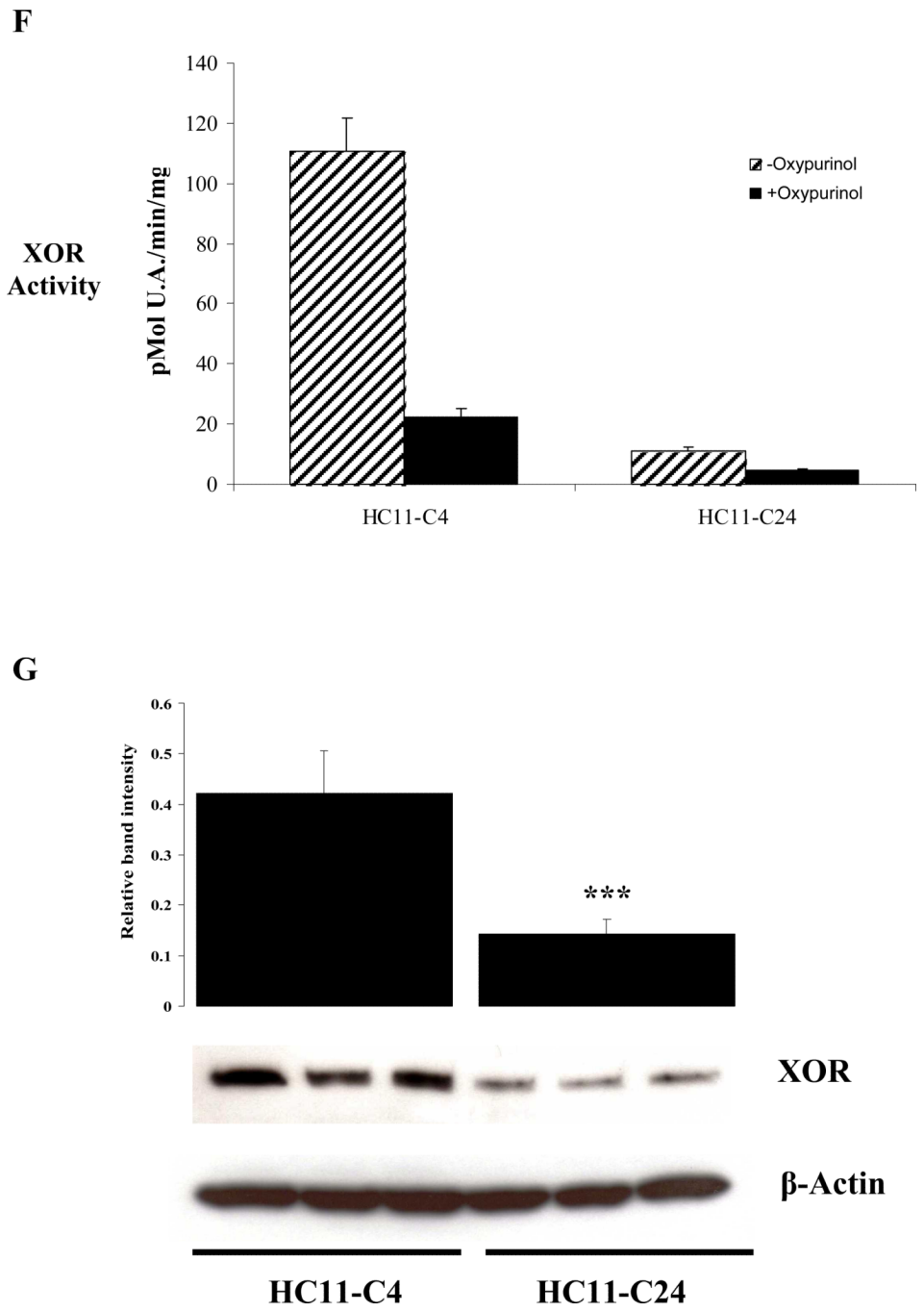

FIGURE 4. Clonally selected HC11-C24 cells exhibit high migration and reduced XOR expression

A, HC11-C4 and HC11-C24 cells were grown on glass coverslips to 80% confluency, treated with TGFβ, and 24hrs later were stained with Alexa Fluor 488 phalloidin, and photographed. *B/C*, HC11-C4 and HC11-C24 cells were grown as indicated above. Cells were then treated as described in the lane designation below, lysed in RIPA buffer, and western blots performed (*C*) against α-SMA or β-Actin and quantitated by scanning dosimetry (*B*). Lane 1, 1 day of growth without TGFβ; lane 2, 9 days of growth without TGFβ; lane 3, 6hrs growth after 5ng/ml TGF-β1; lane 4, 12hrs after TGFβ1; lane 5, 1 day after TGF-β1; lane 6, 2 days after TGF-β1; lane 7, 3 days after TGF-β1; lane 8, 9 days after

NIH-PA Author Manuscript

NIH-PA Author Manuscript

NIH-PA Author Manuscript

TGF-β1; lane 9, 12hrs without TGFβ. Band intensity was quantitated using Kodak Imager software, and relative intensities normalized to the signal obtained with β-Actin (*B*). *D/E,* HC11-C4 and HC11-C24 were grown to confluency, wounded with a plastic pipette tip, and washed three times in PBS to remove floating cells. Medium was then replaced with standard growth medium containing 10% heat inactivated FCS, and 5.0 ng/ml TGFβ was added or not as indicated. Cells were photographed at 0, 19, and 31hrs after the addition of TGFβ. Migration was quantitated by open surface area calculation (*D*), and representative photomicrographs are shown for each time point (*E*). *F*, HC11-C4 and HC11-C24 were grown to confluency in six well plates, cells were harvested three days later, and XOR activity was determined. Data show the mean and standard deviation of six determinations. *G*, western immunoblot analysis was performed on the whole cell extracts used in panel F, and three representative lanes are shown for both cell types.

NIH-PA Author Manuscript

NIH-PA Author Manuscript

NIH-PA Author Manuscript

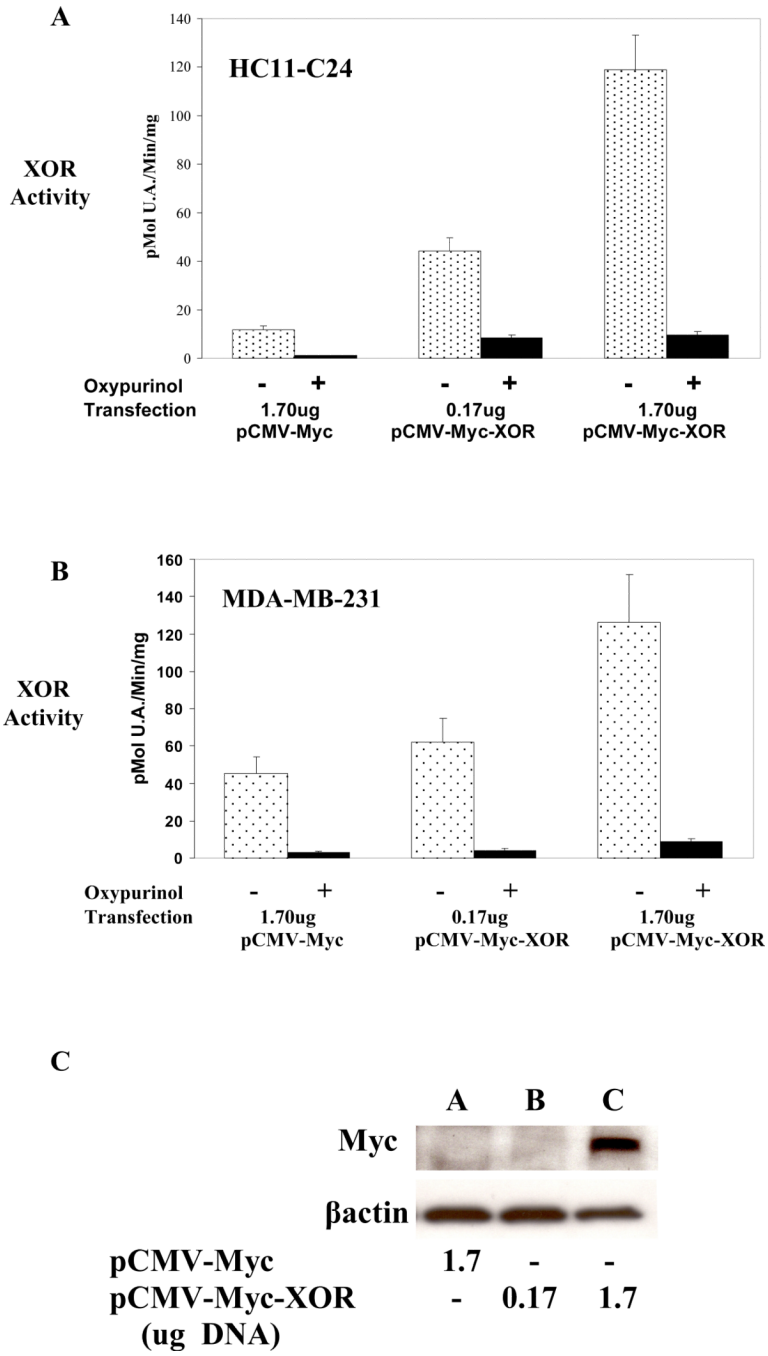

NIH-PA Author Manuscript

NIH-PA Author Manuscript

NIH-PA Author Manuscript

D

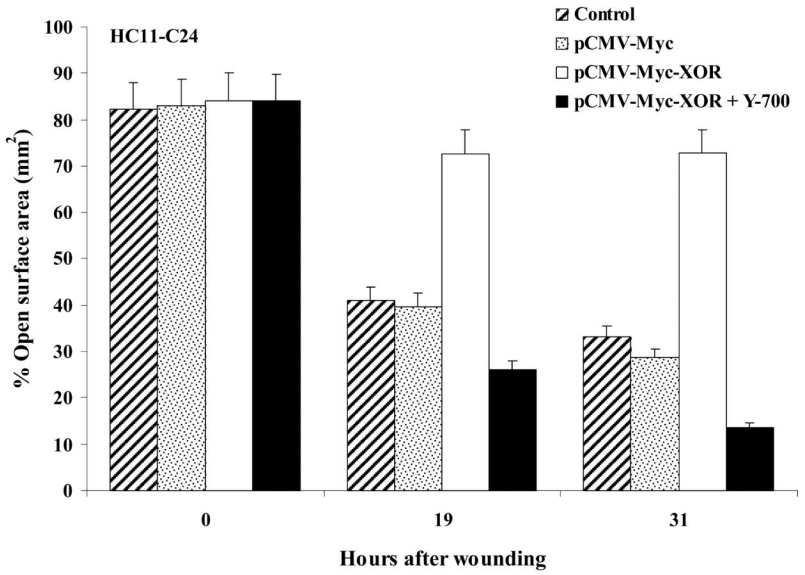

E

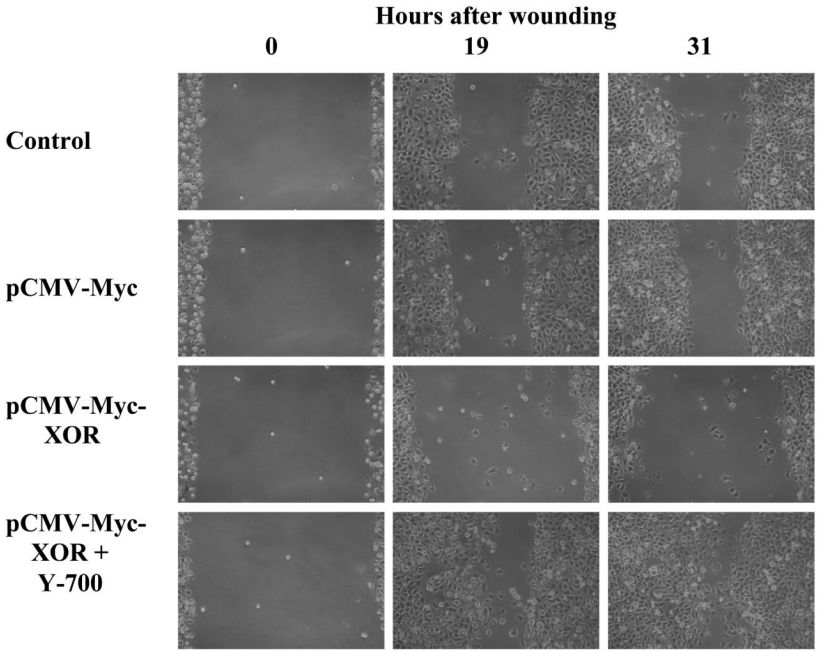

NIH-PA Author Manuscript

NIH-PA Author Manuscript

NIH-PA Author Manuscript

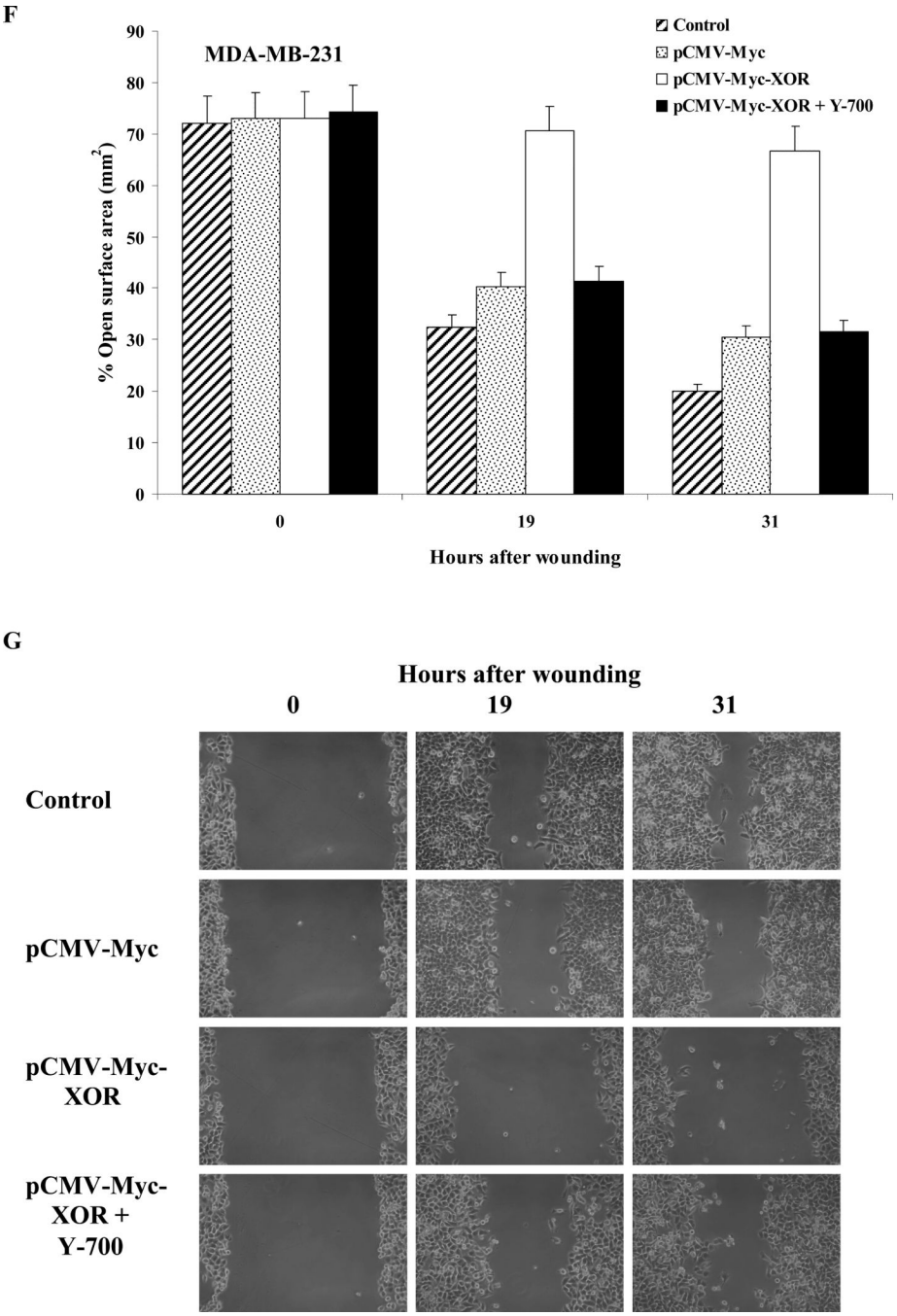

FIGURE 5. Over-expression of recombinant XOR cDNA inhibits migration in HC11-C24 and MDA-MB-231 MEC *in vitro*

A, pCMV-Myc-XOR or the pCMV-Myc empty vector were transfected into HC11-C24 in six well plates at the indicated DNA levels, cells were harvested after 24hrs, and oxypurinol inhibitable XOR activity was determined. *B*, pCMV-Myc-XOR or the pCMV-Myc empty vector were transfected into MDA-MB-231 in six well plates at the indicated DNA levels, cells were harvested after 24hrs, and oxypurinol inhibitable XOR activity was determined. Data show the mean and standard deviation of six independent determinations in both panels. *C*, western immunoblot of Myc-tagged XOR for the XOR activity data shown in panel *B*. *D*, Quantitation of migration in HC11-C24. pCMV-Myc-XOR or the pCMV-Myc

NIH-PA Author Manuscript

NIH-PA Author Manuscript

NIH-PA Author Manuscript

empty vector were transfected into HC11-C24 in the presence or absence of the XOR inhibitor Y-700. The effect on migration was quantitated at 0, 19, and 31hrs later using open surface area determination. *E*, representative photomicrographs are shown for the migration assay in panel *D*. *F*, migration quantitation in MDA-MB-231. pCMV-Myc-XOR or the pCMV-Myc empty vector were transfected into MDA-MB-231 in the presence or absence of Y-700. The effect on migration was quantitated 0, 19, and 31hrs later by open surface area calculation. *G*, representative photomicrographs are shown for the wound assay in panel *E*.

NIH-PA Author Manuscript

NIH-PA Author Manuscript

NIH-PA Author Manuscript

A

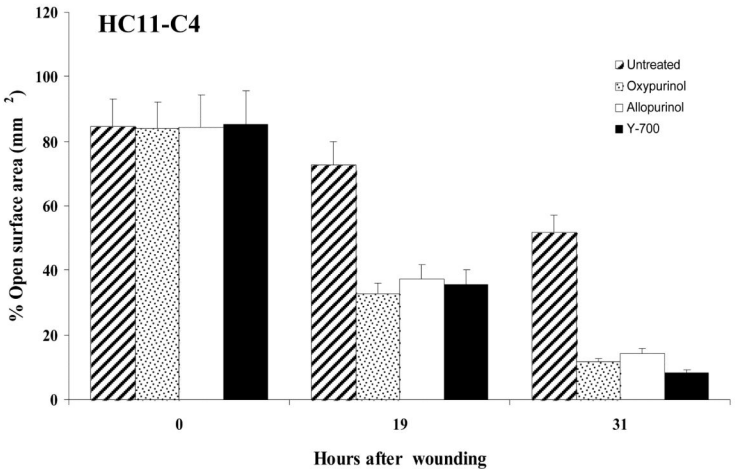

B

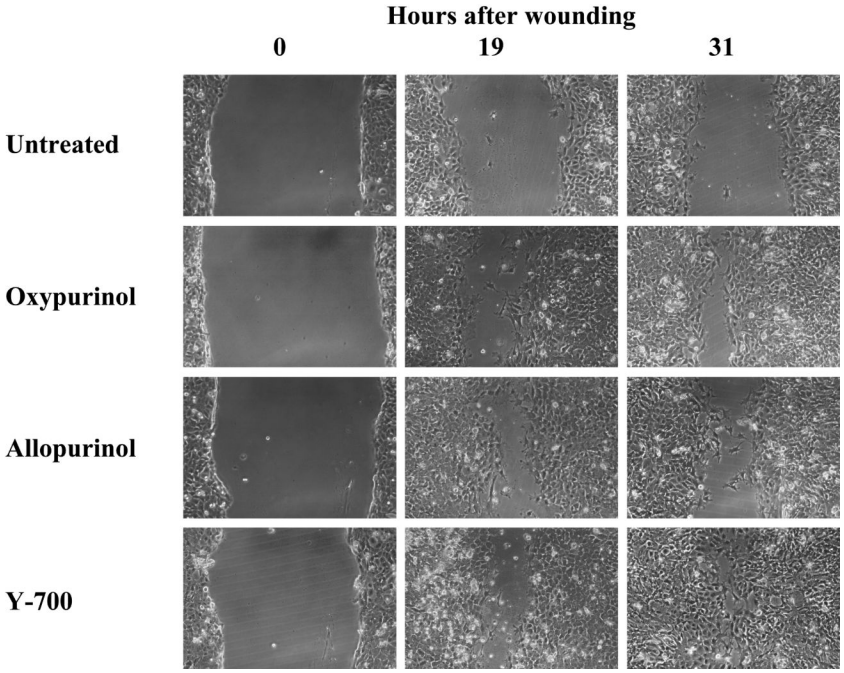

NIH-PA Author Manuscript

NIH-PA Author Manuscript

NIH-PA Author Manuscript

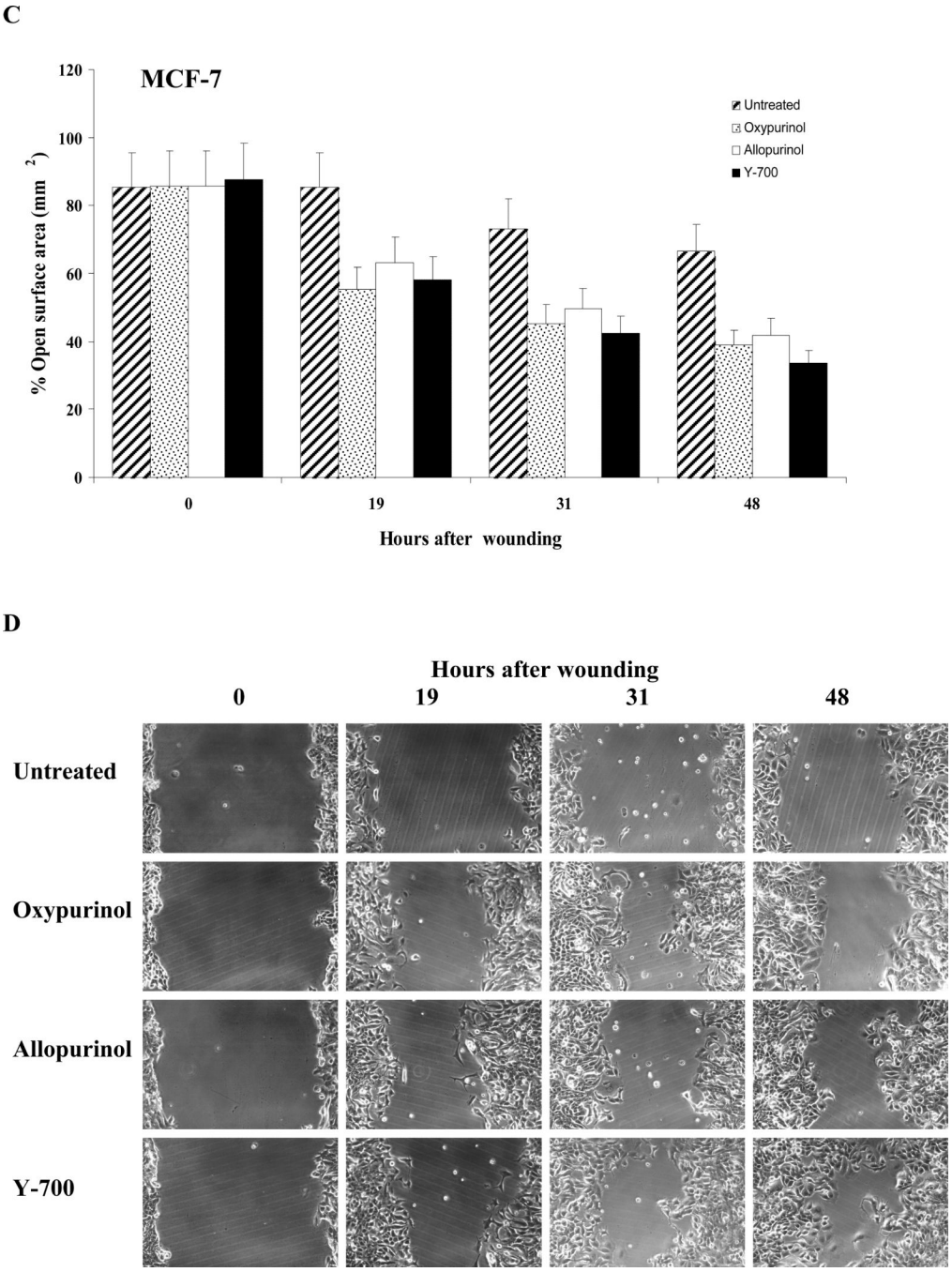

FIGURE 6. Inhibition of XOR stimulates migration in HC11-C4 mouse and MCF-7 human MEC *in vitro*

A, HC11-C4 mouse MEC were grown to confluency and treated with either oxypurinol (150uM, stippled), allopurinol (150uM, open), Y-700 (1uM, black), or remained untreated (hatched). After one hour, cells were subjected to wounding, washed, and the medium refreshed in the presence of XOR inhibitors. Migration was quantitated 0, 19, and 31hrs after wounding using surface area calculation. Data show the mean and standard deviation of six independent assays. *B*, representative photomicrographs are shown for each time point. *C*, MCF-7 human MEC were grown to confluency, treated as above, and migration was quantitated 0, 19, 31, and 48hrs after wounding using surface area calculation. Data

show the mean and standard deviation of six independent assays. *D*, representative photomicrographs are shown for each time point.

NIH-PA Author Manuscript

NIH-PA Author Manuscript

NIH-PA Author Manuscript

NIH-PA Author Manuscript

NIH-PA Author Manuscript

NIH-PA Author Manuscript

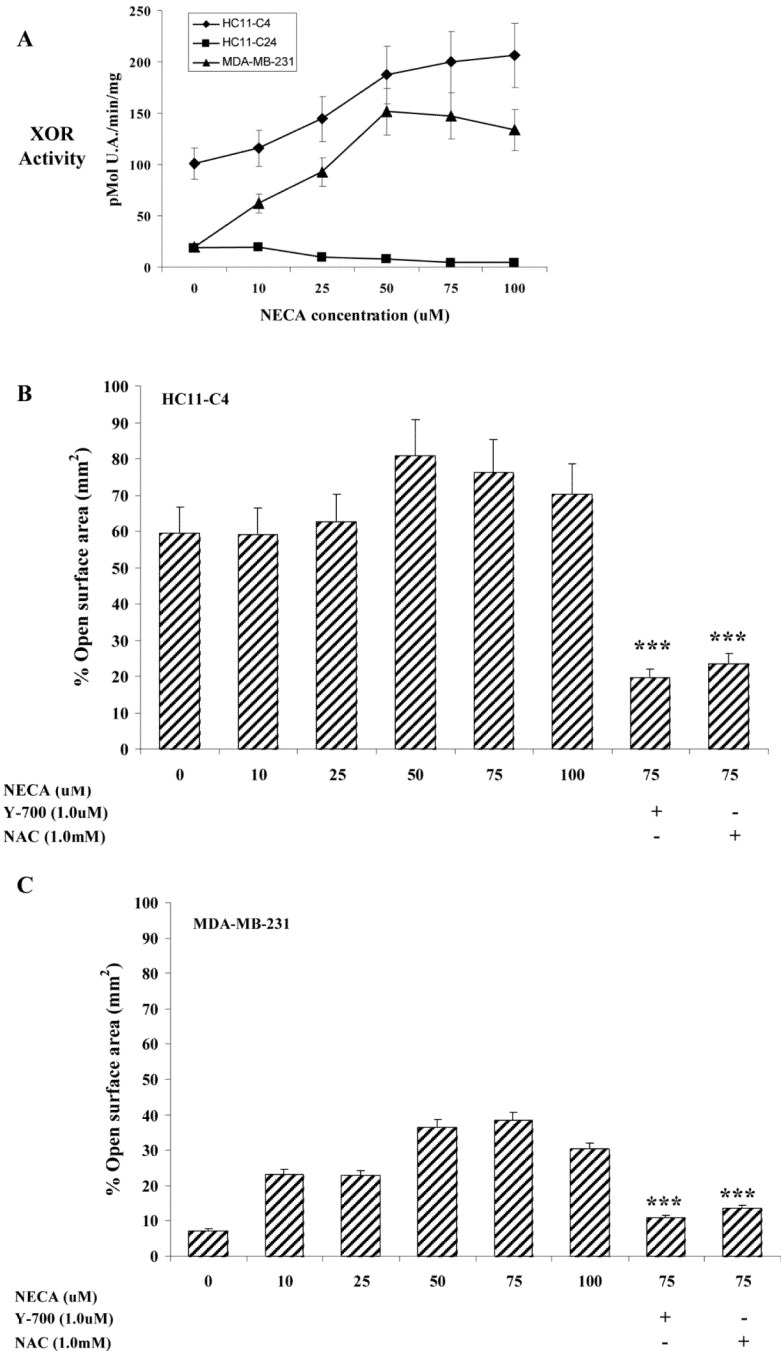

NIH-PA Author Manuscript

NIH-PA Author Manuscript

NIH-PA Author Manuscript

D

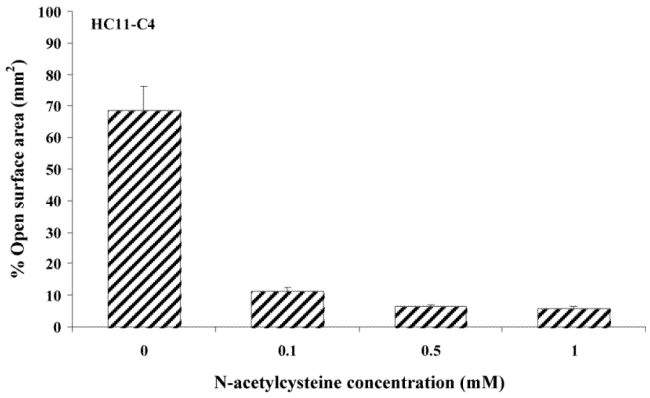

E

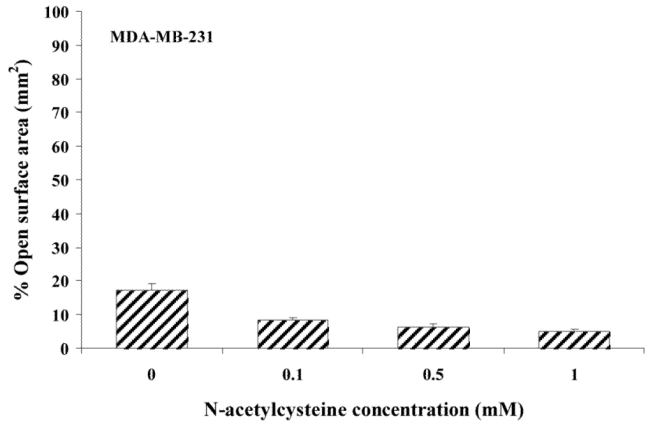

F

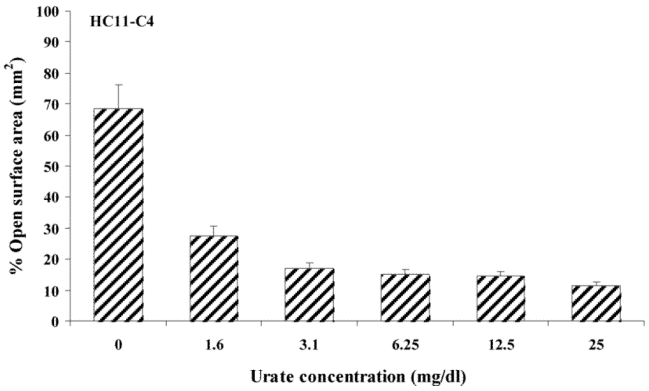

NIH-PA Author Manuscript

NIH-PA Author Manuscript

NIH-PA Author Manuscript

G

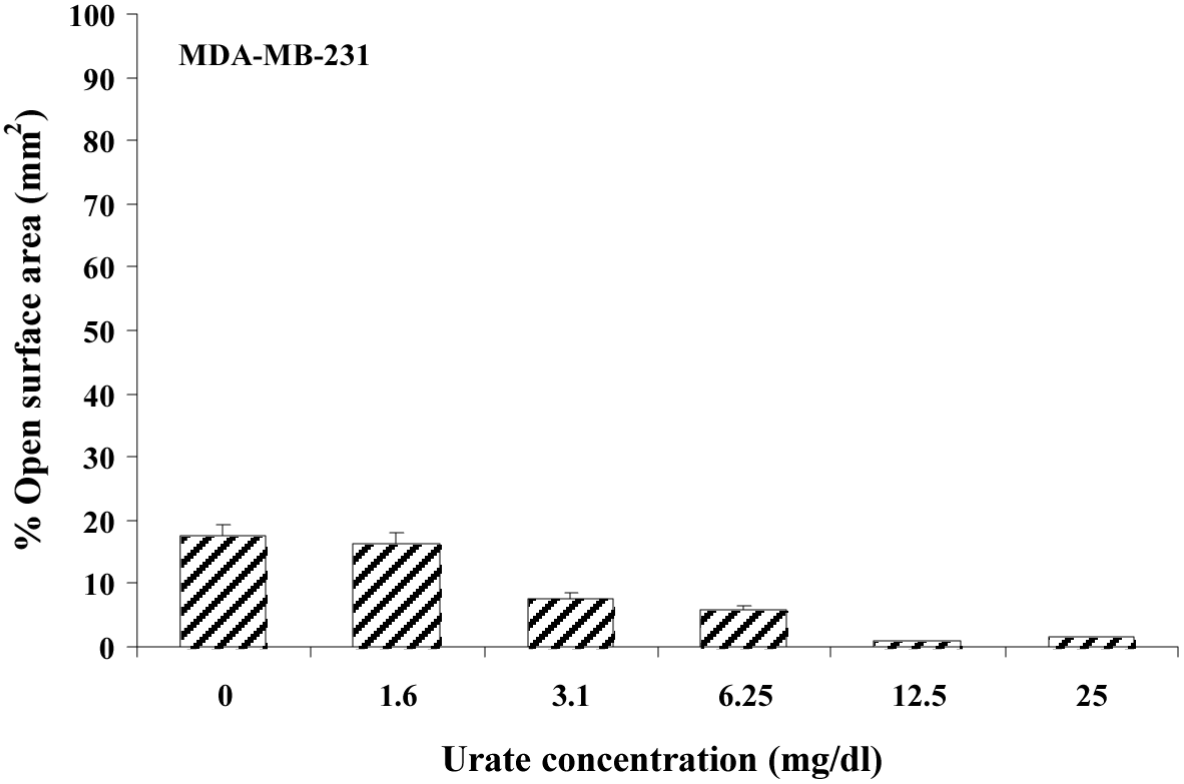

FIGURE 7. XOR derived ROS may contribute to suppression of MEC migration *in vitro*

A, HC11-C4, HC11-C24, and MDA-MB-231 cells were grown to confluency and treated with NECA at the indicated doses. XOR activity was determined 48hrs later. Data show the mean and standard deviation of four repetitions each. *B*, *C*, HC11-C4 MEC (B) or MDA-MB-231 (C) were grown to confluency and treated with either Y-700, N-acetylcysetine (NAC), or remained untreated. After one hour, cells were subjected to wounding, washed, and the medium refreshed in the presence of Y-700 or NAC, and NECA was added at the indicated doses. Migration was quantitated 19hrs (HC11-C4) or 48hrs (MDA-MB-231) after wounding using surface area calculation. Data show the mean and standard deviation of six independent assays. ***, $p < 0.001$ by Students T-test. *D*, *E* HC11-C4 (D) and MDA-MB-231 (E) cells were grown to confluency and treated with NAC at the indicated doses. After one hour, cells were subjected to wounding, washed, and the medium refreshed in the presence of NAC at the indicated doses. Migration was quantitated 19hrs (HC11-C4) or 48hrs (MDA-MB-231) after wounding using surface area calculation. Data show the mean and standard deviation of six independent assays. *F*, *G* HC11-C4 (F) and MDA-MB-231 (G) cells were grown to confluency and treated with urate at the indicated doses. After one hour, cells were subjected to wounding, washed, and the medium refreshed in the presence of urate at the indicated doses. Migration was quantitated 19hrs (HC11-C4) or 48hrs (MDA-MB-231) after wounding using surface area calculation. Data show the mean and standard deviation of six independent assays.

NIH-PA Author Manuscript

NIH-PA Author Manuscript

NIH-PA Author Manuscript

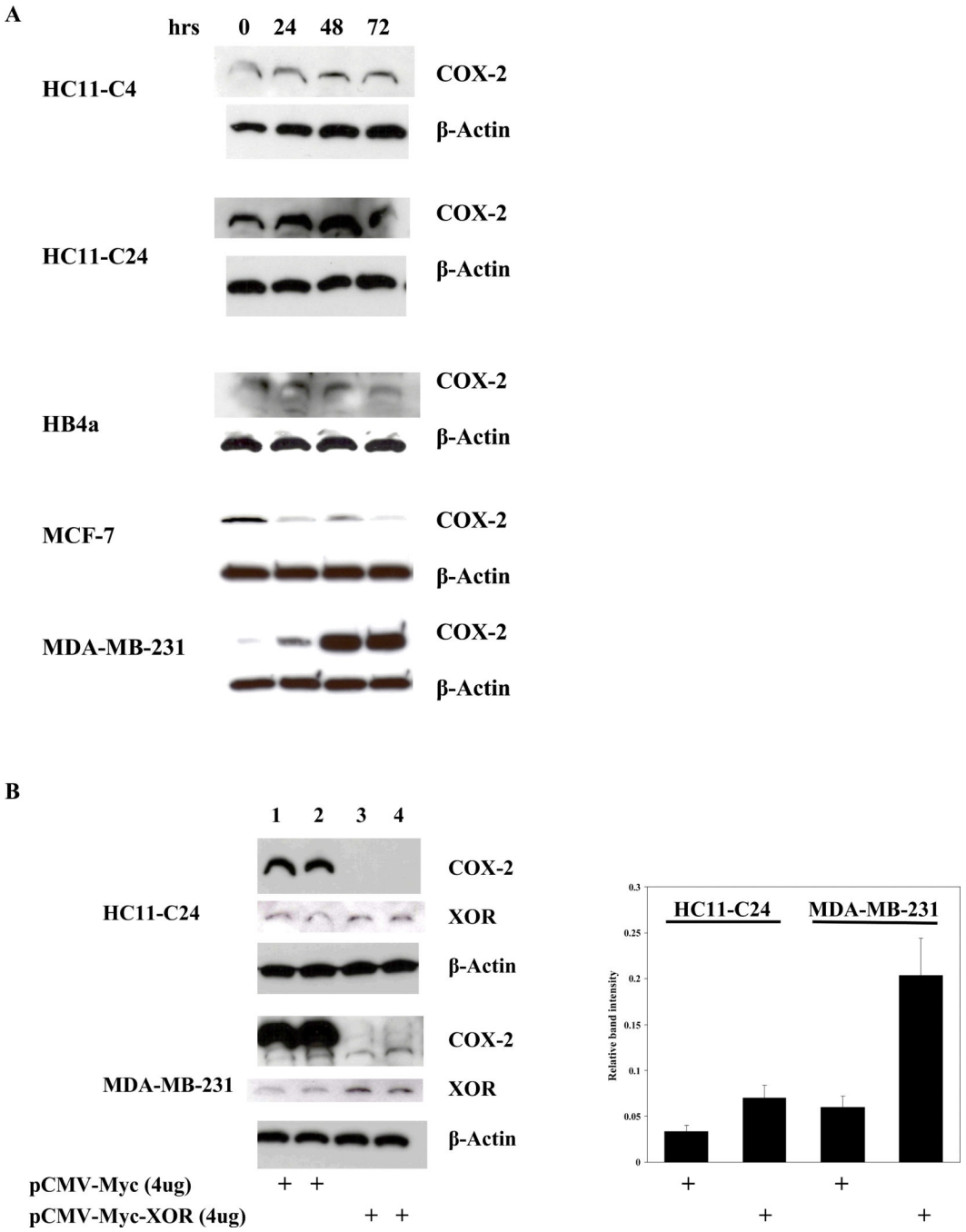

NIH-PA Author Manuscript

NIH-PA Author Manuscript

NIH-PA Author Manuscript

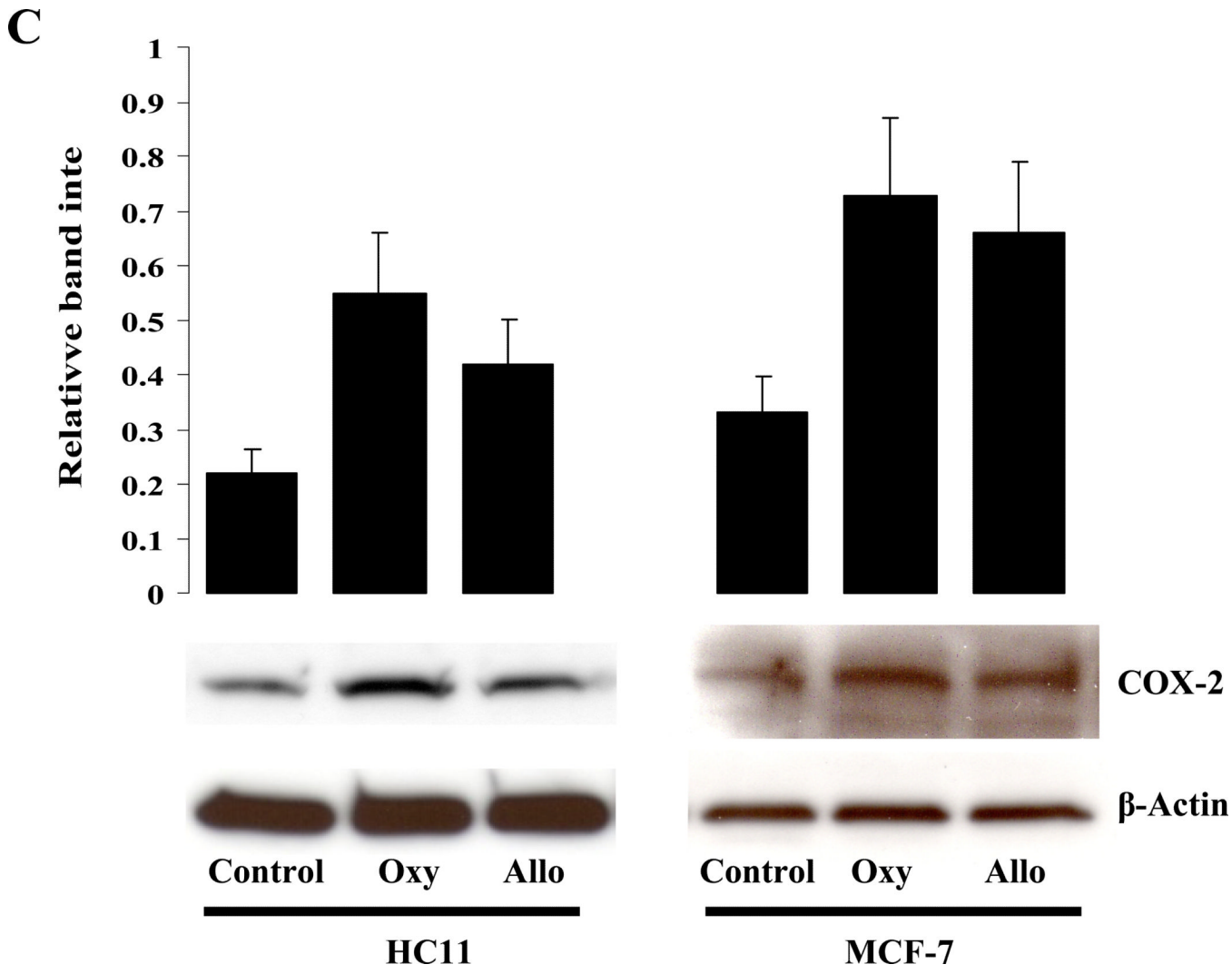

FIGURE 8. XOR contributes to COX-2 regulation in carcinoma and normal MEC

A, The indicated MEC were grown to confluence and harvested every 24hrs over the subsequent 72hrs. Whole cell extracts were prepared and used for western blot analysis of COX-2 and β-Actin, which was used to standardize loading of the gels. All samples were run in triplicate, and representative blots are shown for each. *B*, HC11-C24 and MDA-MB-231 were transfected in six well plates with 4.0 ug of either pCMV-Myc vector (lanes1 and 2) or pCMV-Myc-XOR (lanes 3 and 4). Whole cell extracts were prepared 48 hours after transfection and western blots were analyzed for COX-2 expression and β-Actin. Duplicate samples were analyzed for each, and XOR protein levels were quantitated by scanning dosimetry and normalized to the β-Actin signal. *C*, HC11 and MCF-7 cells were plated in six well plates at 35% confluency. After 24hrs cells were treated with either oxypurinol or allopurinol at 150uM. Whole cell extracts were prepared 24hrs later and analyzed for expression of COX-2 and β-Actin. Band intensity was quantitated by scanning dosimetry. Samples were prepared in triplicate and representative blots are shown.

NIH-PA Author Manuscript

NIH-PA Author Manuscript

NIH-PA Author Manuscript

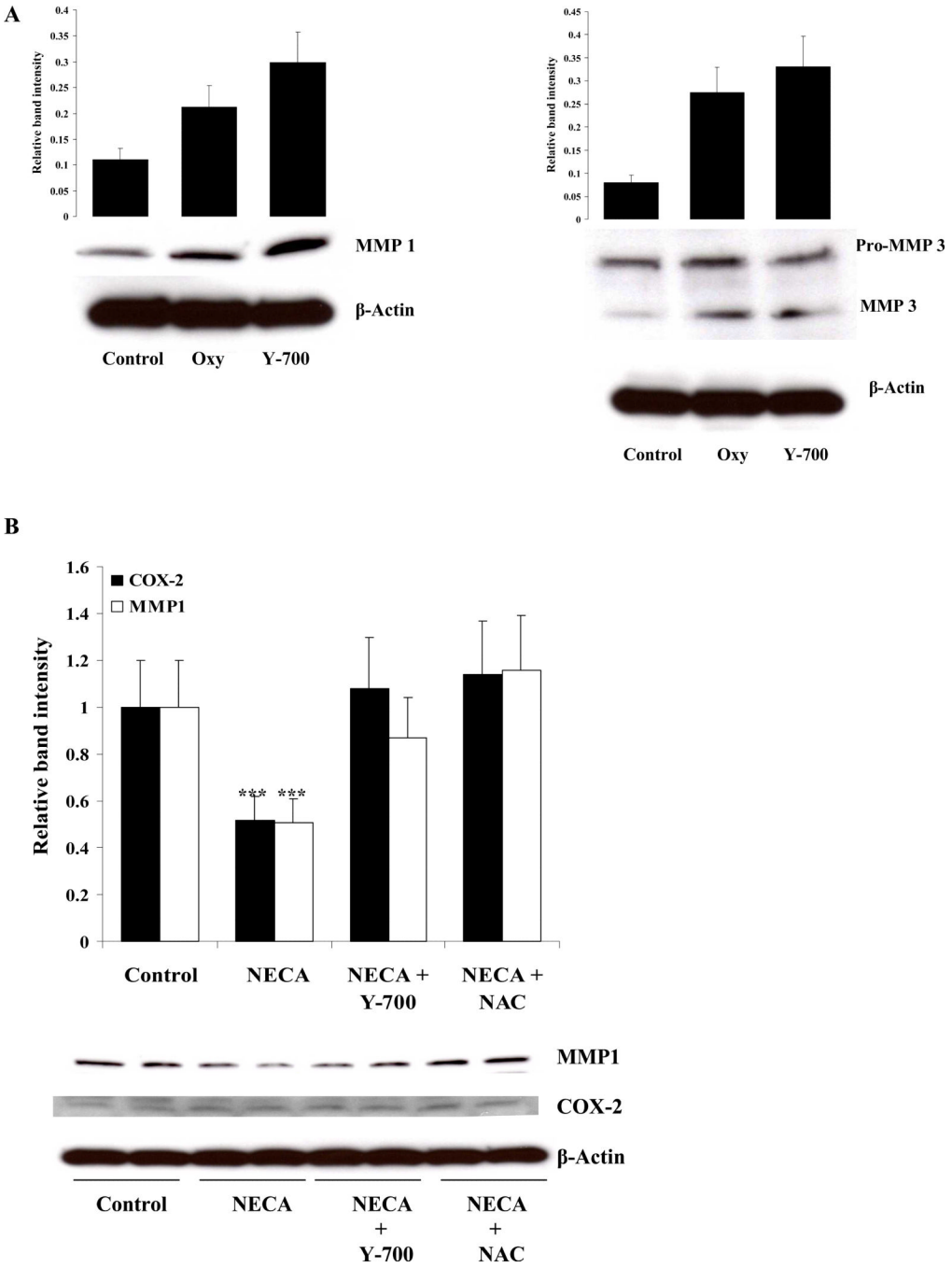

NIH-PA Author Manuscript

NIH-PA Author Manuscript

NIH-PA Author Manuscript

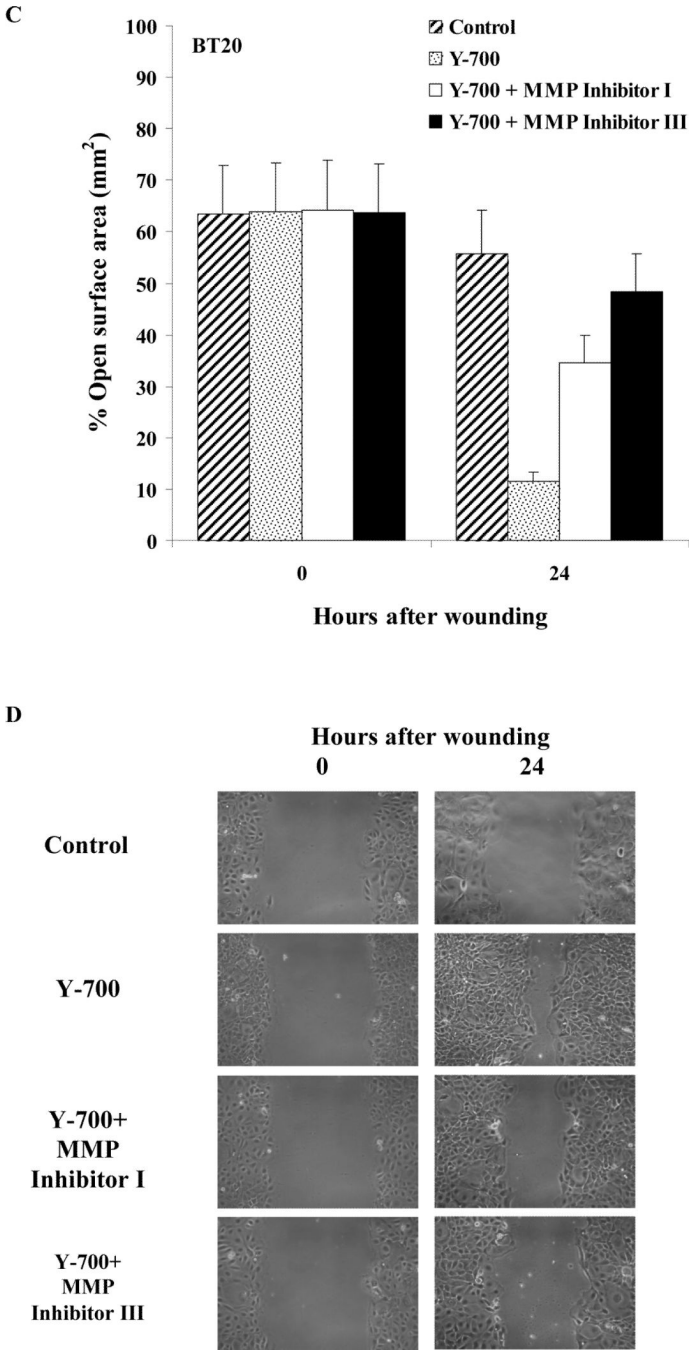

FIGURE 9. XOR modulates MMP protein levels and function in human carcinoma cells

A, MDA-MB-231 cells were grown to confluency in six well plates and treated with either oxypurinol or Y-700. After 72hrs of growth whole cell extracts were prepared and analyzed by western blot for expression of MMP1, MMP3, and β-Actin. Band intensities of the mature, active MMP1 and MMP3 were quantitated by scanning dosimetry and normalized to the actin signal. *B*, MDA-MB-231 cells were grown as above and treated with either Y-700 at a dose of 1.0uM, NAC at a dose of 1mM, or untreated (control). NECA was added 1hr later at a dose of 50uM. Whole cell extracts were prepared 24hrs later and western blots analyzed for COX-2, MMP1, and β-Actin. All samples were run in duplicate. Band intensities (top panel) were quantitated by scanning dosimetry for the gels shown in the

NIH-PA Author Manuscript

NIH-PA Author Manuscript

NIH-PA Author Manuscript

lower panel and normalized to the control signal. *** $p < 0.02$ by Students t-Test. *C*, Quantitation of migration in the human carcinoma cell line BT20. Cells were grown to confluency in 12 well trays, wounded, and treated as indicated with either the XOR inhibitor Y-700, Y-700 in combination with MMP inhibitor I (150uM), or Y-700 in combination with MMP inhibitor III (150nM). Migration was quantitated 0 and 24hrs after wounding using open surface area calculation. Data show the mean and standard deviation of six determinations for each treatment. *D*, representative photomicrographs are shown for each treatment group shown in panel *C*.

NIH-PA Author Manuscript

NIH-PA Author Manuscript

NIH-PA Author Manuscript

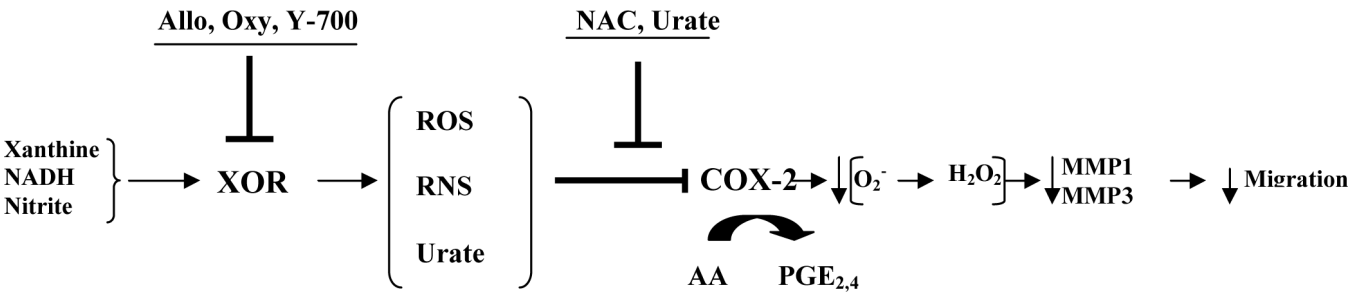

FIGURE 10. A possible mechanism for the contribution of XOR to modulation of MEC migratory activity and to COX-2 and MMP expression

The postulated situation obtained in cells exhibiting high XOR and weak COX-2 expression is illustrated. Xanthine, NADH, and nitrites are the three substrates most likely used by XOR in MEC. Allopurinol (Allo), Oxypurinol (Oxy), and Y-700 are XOR specific inhibitors. XOR can generate the ROS $O^{-\cdot}_2$ and H_2O_2 during catalysis. NO can be generated directly from XOR catalysis during nitrite metabolism, contributing to RNS generation. Urate will be formed by XOR following xanthine oxidation. We posit that XOR derived ROS, RNS, or urate may contribute to modulation of COX-2. When COX-2 levels are sufficiently high, it is imagined that COX-2, possibly through and ROS based mechanism, stimulates MMP1/MMP3 levels contributing to migratory activity. Modulation of COX-2 by high level XOR activity is then imagined to reduce MMP1/MMP3 and migratory activity. AA, arachidonic acid; PGE, prostaglandin; NAC, N-acetylcysteine.

NIH-PA Author Manuscript

NIH-PA Author Manuscript

NIH-PA Author Manuscript

Table 1

Selected characteristics of HC11-C4 and HC11-C24 cells are shown. *, spontaneous cell death rate was determined after growing cells in standard rich medium containing 10% FCS and then shifting the cells into serum free medium (SFM). Cells were grown for 48hrs following the shift into SFM and spontaneous cell death was determined following trypsinization and washing using Trypan Blue exclusion and manual counting with a hemocytometer. #, doubling time for each cell line was determined by plating at a density of 3.0×10^5 cells per well in six well trays. Trypsinized cells were counted manually 24 and 48 hours later using a hemocytometer. Response to TGFβ was determined by western immunoblot (α-SMA, E-cadherin) as shown above or by visual inspection of photomicrographs (phalloid stain for F-actin fiber formation). XOR activity was determined as shown in Fig. 4F.

Comparison of Characteristics

	HC11-C4	HC11-C24
Spontaneous cell death*	**21%**	**22%**
Doubling time#	**25 hrs**	**19 hrs**
TGF_β response:		
F-Actin stress fiber formation	**No**	**Yes**
α-SMA expression	+	+ + + +
E-Cadherin expression	+ +	+ + + +
XOR activity (pMol U.A./min/mg)	**109 +/− 6.76**	**16.2 +/− 1.16**